

Computational Analysis of Heat Wave and its Mitigation in an Urban Microclimate



Moiz Mohsin

205318

Dr. Zaib Ali

DEPARTMENT: SCHOOL OF MECHANICAL & MANUFACTURING
ENGINEERING

NATIONAL UNIVERSITY OF SCIENCES AND TECHNOLOGY

ISLAMABAD

JANUARY , 2020

Computational Analysis of Heat Wave and its Mitigation in an Urban Microclimate

Moiz Mohsin

205318

A thesis submitted in partial fulfillment of the requirements for the degree of
MS Mechanical Engineering

Thesis Supervisor:

Dr. Zaib Ali

Thesis Supervisor's Signature:



DEPARTMENT

SCHOOL OF MECHANICAL & MANUFACTURING ENGINEERING


NATIONAL UNIVERSITY OF SCIENCES AND TECHNOLOGY,

ISLAMABAD

JANUARY, 2020


THESIS ACCEPTANCE CERTIFICATE

It is certified that final copy of MS/MPhil thesis written by Mr. Moiz Mohsin Registration No. 00000205318 of SMME has been vetted by undersigned, found complete in all aspects as per NUST Statutes/Regulations, is free of plagiarism, errors, and mistakes and is accepted as partial fulfillment for award of MS/MPhil degree. It is further certified that necessary amendments as pointed out by GEC members of the scholar have also been incorporated in the said thesis.

Signature with stamp:  Assistant Professor
School of Mechanical and
Manufacturing Engineering
(SMME) NUST, Islamabad.

Name of Supervisor: **Dr. Zaib Ali**

Date:

Signature of HoD with stamp:  DR. EMAD UDDIN
HoD Mech Engg.
School of Mechanical &
Manufacturing Engineering (SMME)
NUST, H-12, Islamabad

Date:

Countersign by

Signature (Dean/Principal): _____

Date: _____

National University of Sciences & Technology

We hereby recommend that the dissertation prepared under our supervision by: (Student Name & Regn No.) Moiz Mohsin 205318 Titled: Computational Analysis of Heat Wave and its Mitigation in an Urban Microclimate be accepted in partial fulfillment of the requirements for the award of Masters degree with (A_Grade).

Examination Committee Members

1. Name: Dr. Emad uddin Signature: 

2. Name: Dr. M. Sajid Signature: 

3. Name: Dr. Sami Ur Rehman Signature: 

Supervisor's name: Dr. Zaib Ali Signature: 
Date: 08/07/2020


Head of Department

08/07/2020
Date

COUNTERSIGNED

Date: _____

Dean/Principal

Declaration

I certify that this research work titled “*Computational Analysis of Heat Wave and its mitigation in an Urban Microclimate*” is my own work. The work has not been presented elsewhere for assessment. The material that has been used from other sources it has been properly acknowledged / referred.

A handwritten signature in black ink, appearing to read 'Moiz Mohsin', written in a cursive style.

Signature of Student

Moiz Mohsin

2017-NUST-MS-Mech-205318

Plagiarism Certificate (Turnitin Report)

This thesis has been checked for Plagiarism. Turnitin report endorsed by Supervisor is attached.



Signature of Supervisor



Signature of Student

Moiz Mohsin

205318

Certificate for Plagiarism

It is certified that ~~PhD/M.Phil~~/MS Thesis Titled **Computational Analysis of Heat Wave and its Mitigation in an Urban Microclimate** ___ by ___Moiz Mohsin has been examined by us. We undertake the follows:

- a. Thesis has significant new work/knowledge as compared already published or are under consideration to be published elsewhere. No sentence, equation, diagram, table, paragraph or section has been copied verbatim from previous work unless it is placed under quotation marks and duly referenced.
- b. The work presented is original and own work of the author (i.e. there is no plagiarism). No ideas, processes, results or words of others have been presented as Author own work.
- c. There is no fabrication of data or results which have been compiled/analyzed.
- d. There is no falsification by manipulating research materials, equipment or processes, or changing or omitting data or results such that the research is not accurately represented in the research record.
- e. The thesis has been checked using TURNITIN (copy of originality report attached) and found within limits as per HEC plagiarism Policy and instructions issued from time to time.

Name & Signature of Supervisor

Dr. Zaib Ali



Signature:

Assistant Professor
School of Mechanical and
Manufacturing Engineering
(SMME) NUST, Islamabad.

Copyright Statement

- Copyright in text of this thesis rests with the student author. Copies (by any process) either in full, or of extracts, may be made only in accordance with instructions given by the author and lodged in the Library of NUST School of Mechanical & Manufacturing Engineering (SMME). Details may be obtained by the Librarian. This page must form part of any such copies made. Further copies (by any process) may not be made without the permission (in writing) of the author.
- The ownership of any intellectual property rights which may be described in this thesis is vested in NUST School of Mechanical & Manufacturing Engineering, subject to any prior agreement to the contrary, and may not be made available for use by third parties without the written permission of the SMME, which will prescribe the terms and conditions of any such agreement.
- Further information on the conditions under which disclosures and exploitation may take place is available from the Library of NUST School of Mechanical & Manufacturing Engineering, Islamabad.

Acknowledgements

I am thankful to my Creator Allah Subhana-Watala to have guided me throughout this work at every step and for every new thought which You setup in my mind to improve it. Indeed, I could have done nothing without Your priceless help and guidance. Whosoever helped me throughout the course of my thesis, whether my parents or any other individual was Your will, so indeed none be worthy of praise but You.

I am profusely thankful to my beloved parents who raised me when I was not capable of walking and continued to support me throughout in every department of my life.

I would also like to express special thanks to my supervisor Dr. Zaib Ali for his help throughout my thesis and also for CFD courses which he has taught me. I can safely say that I haven't learned any other engineering subject in such depth than the ones which he has taught.

I would also like to pay special thanks to my wife for her tremendous support and cooperation. I appreciate her patience and support throughout the whole thesis.

Finally, I would like to express my gratitude to all the individuals who have rendered valuable assistance to my study.

*Dedicated to my exceptional parents, sister and my wife whose
tremendous support and cooperation led me to this wonderful
accomplishment.*

Abstract

Climate change is having various kinds of adverse effects on the society and the environment. The frequency of summer-time heat waves is increasing and Urban Heat Island Effect can significantly affect the local microclimate which consequently escalates human mortality and mortality. Most of the studies performed in this area are employing field measurements and observational methods which is inadequate to predict the urban temperatures, deterministic approach is required in order to completely forecast the thermal environment. In this study, a computational fluid dynamics simulation of an urban micro-climate during a period of heatwave is performed. 3D unsteady Reynolds-averaged Navier Stokes (URANS) simulations with the realizable k- ϵ turbulence model are performed on high-resolution computational grid. Various climate variables such as surface temperature, wind velocity and air temperature have been calculated. The CFD surface temperature data is compared with the Satellite Data from the MODIS product of the June-2015 heatwave period in Karachi in the year 2015. A reasonable agreement of the simulated data with the satellite recorded data has been obtained. It is therefore concluded that CFD has the prospect to precisely determine the urban surface temperature with deviation of around 10% from the satellite data. Moreover, as a climate adaptation measure, the effect of albedo or decreased surface absorptivity on the outdoor environment is simulated. It has been observed that high albedo can decrease the temperature up to 2°C, thus decreasing the heat stress.

Keywords: CFD, climate change adaptation, urban heat island, urban microclimate

Contents

Declaration.....	i
Plagiarism Certificate (Turnitin Report).....	ii
Copyright Statement.....	iv
Acknowledgements	v
Abstract.....	vi
List of Figures.....	ix
List of Tables	x
1. Introduction.....	1
1.1 Micro-climate and Heat Waves	1
1.2 Urban Heat Islands	3
1.3 Heat Waves in Pakistan.....	4
1.4 Description of Microclimate.....	5
1.5 Research Methodology	7
2. Literature Review	8
3. Numerical Methods.....	14
3.1 Methodology	14
3.1.1 Target Variables.....	14
3.1.2 Models for Computation	14
3.2 Geometry	14
3.2.1 Domain of Generic Urban Area.....	15
3.2.2 Domain of Real Urban Area	16
3.2.2 Computational Grid.....	18
3.3 Initial and Boundary Conditions	20
3.3.1 Boundary Conditions.....	20
3.3.2 Aerodynamic Roughness Length	21
3.4 Solution Methods and Controls	22
3.4.1 Numerical Approximations	22
3.5 Thermal Model.....	22
3.6 Settings Table for Computation.....	23
4. Results: CFD Simulation of Microclimate.....	25
4.1 Validation of Surface Temperatures	25
4.1.1 Satellite Measurements of Surface Temperature	25
4.1.2 Validation Study.....	27
4.1.2.1 Measured Meteorological Conditions	27

4.1.2.2 Validation Study of Wind Flow	29
4.1.3 Results and Comparison (Real Urban Area).....	30
5. Mitigation Measures	33
5.1 Cool Pavement Materials	34
6. Discussion.....	36
6.1 Urban Geometry and Mesh.....	36
6.2 Wind Flow, Solar Radiation and Thermal Model.....	36
6.3 Albedo as a Mitigation Measure	37
6.4 Recommendations for further Research.....	37
7. Conclusion	38
References.....	39
Appendix.....	43

List of Figures

Figure 1: Temperature Anomaly globally from 1880 to 2020.....	1
Figure 2: Effects and Mechanisms for heatwaves [2].....	2
Figure 3: June-August Temperature Anomalies (relative to 1961-1990 mean) over the shown region. European Map and effect of heatwaves is represented on the left top corner.....	3
Figure 4: a) Heat Index Anomalies in Pakistan b) Maximum Temperature and Relative humidity Anomalies for the Period 1961-2007 [12].....	4
Figure 5: Karachi Heat Index from 17 to 24th June,2015 [14].....	5
Figure 6:Urban Microclimate, Karachi Aerial View [15].....	6
Figure 7: Single Building Model with a Passage.....	15
Figure 8: Computational Grid of Single Building with the Passage (PointWise).....	16
Figure 9: Computational Grid of Passage in a Single Building.....	16
Figure 10: Computational Domain of Real Urban Area.....	17
Figure 11: Satellite Image of the Urban Area Domain.....	17
Figure 12: Ground Plane Model of Urban Microclimate, Karachi.....	18
Figure 13: Circular Sub domain in Computational Grid.....	19
Figure 14: Real Urban Domain under study.....	20
Figure 15: Estimated Aerodynamic Roughness Length. Red line Circle is the subdomain and white hexagon is the complete computational domain. Aerodynamic Roughness Length are given according to Davenport Classification.....	22
Figure 16: Average Surface Temperature from MODIS Product from 18th June 2015 to 22 nd June 2015.....	26
Figure 17:Wind Velocity Ratio vs Position in the Passage of building at different Settings.....	29
Figure 18:Representation of Microclimate and 15 Data Points with Temperature Contours 19th June 1300.....	30
Figure 19: 3D View of an Urban Microclimate Surface Temperature 19th June 1300.....	31
Figure 20:Comparative Graph for the model validation results.....	32
Figure 21:Surface Temperature Distribution based on data points used in validation model. Note that average is calculated as 320.54 K.....	33
Figure 22:3D View of Temperature Contours of Mitigated Urban Microclimate 19th June 1300.....	35
Figure 23: Air Temperature vs Time from 18th June to 22nd June 2015.....	45
Figure 24: Wind Speed vs Time from 18th June to 22nd June 2015.....	46

List of Tables

Table 1: Suggested causes of Urban Heat island [10].....	4
Table 2: Previous Studies Review	11
Table 3: Cells count of Computational Grid.....	19
Table 4: CFD Settings.....	23
Table 5: Table of Data acquisition of Satellite Temperatures.....	26
Table 6:Input Data for Selected hours from the Meteorological Department of Karachi.....	27
Table 7:Inlet and Outlet Faces and Walls of the Computational Domain at different orientations	28
Table 8:Using cool pavement materials as a mitigation measure to reduce the surface temperature ...	34

1. Introduction

1.1 Micro-climate and Heat Waves

In recent years, there are two major terms that we have been listening are global warming and climate change. The causes for such drastic changes are many such as industrial activities and automobiles. Temperature anomaly is on the rise as human activity is being increased in this era as shown in Figure 1. There is a growing concern for the people, infrastructure, and ecology of microclimates that are at extreme risk from the harmful effects of climate change. It is proved that the developed areas exert negative influence over their microclimate and thermal discomfort for pedestrians is increased [1].

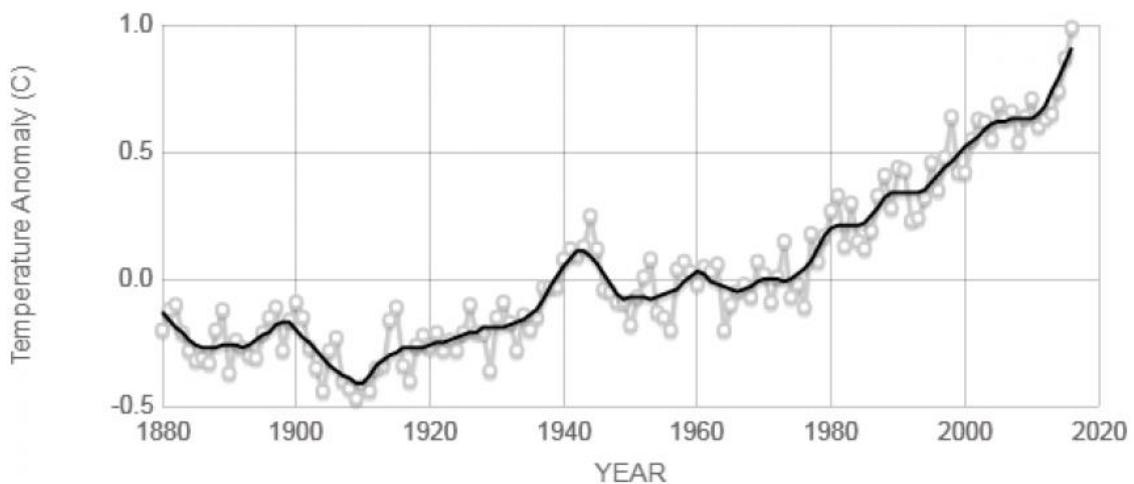


Figure 1: Temperature Anomaly globally from 1880 to 2020

According to the World Meteorological department, the heatwave is defined as “when the maximum day temperature in a week exceeds 5 °C for more than five consecutive days compared to the normal temperature conditions in an area”. Heatwaves are major climatic events that are difficult to forecast and harm the environment and human beings. It is generally considered as the ‘prolonged period of excessive heat’ [2]. Heatwaves have number of consequences which affect buildings and infrastructure, health, cost, society and power consumption due to high energy demand as shown in Figure 2. Robinson figured out that: “there are two aspects of the heat which are either physiological and sociological. The

physiological aspect depends on the general thermoregulation of the human body and the sociological aspect highly relates to local adaptations to the climate [3].

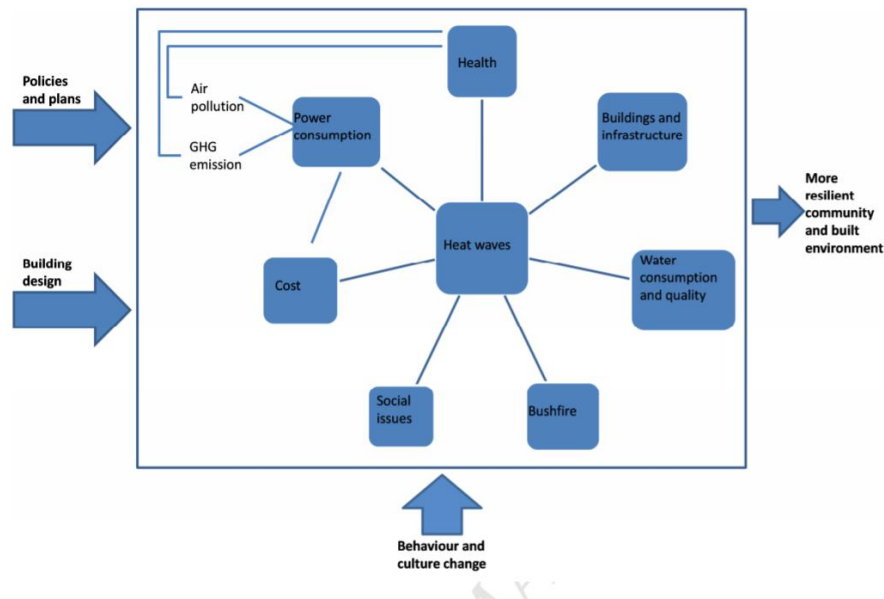


Figure 2: Effects and Mechanisms for heatwaves [2]

As urbanization has increased over time, human influence has almost doubled the risk of heatwave due to industrial activities [4]. In the Figure 3 below, heatwaves of Europe are analyzed over time. An unusually large number of deaths were reported in France, Germany, and Italy. Not only Europe, the temperature of the earth is rising globally and heat waves are seen all over the world at different times and conditions. Most of the UHI effect is observed in the recent decades has been caused by the atmospheric concentrations of greenhouse gases.

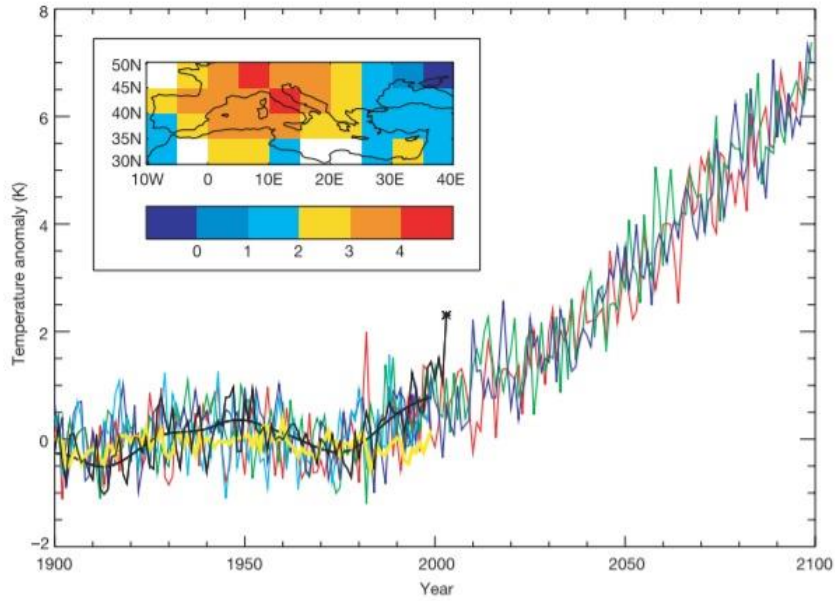


Figure 3: June-August Temperature Anomalies (relative to 1961-1990 mean) over the shown region. European Map and effect of heatwaves is represented on the left top corner

1.2 Urban Heat Islands

The air and surface temperatures of the densely populated urban areas is usually higher than the surrounding environment [5]. During the summers, temperatures in urban centers are 1-6°C are higher than the surrounding rural areas [6]. In the metropolitan cities, the temperature at the center of the cities is often higher than in the suburbs. This is what called as Urban Heat Island Effect. Rural settings tend to shift towards better environments as compared to urban settings where urban canyons, anthropogenic causes, minimal shades of trees, minimal vegetation and plantation, less number of water bodies, and low albedo materials pavements are common. [7]. In 1973, Tim Oke showed that temperature is somehow related to the density of the urban center, and also the temperature increases as the size of the city increases, which creates a severe UHI effect [8]. In 1982, Oke summarized the causes of Urban Heat Island effect which are shown in Table 1. Urban Heat Island effect is due to less turbulent transport in the narrow streets which eventually affects pedestrian's comfort. It is advised to plant trees and do vegetation on the pavements for the thermal comfort of the pedestrians [9].

Table 1: Suggested causes of Urban Heat island [10]

Energy Balance Term responsible for thermal anomaly	Negative Effects due to energy balance changes
Increased absorption of short-wave radiation	Multiple Reflection & increased surface area
Increased long wave radiation from the sky	Greater absorption and re-emission
Decreased long wave radiation loss	Reduction of sky view factor
Anthropogenic Heat Source	Building and Traffic losses
Increased sensible Heat Storage	Increased thermal admittance
Decreased evapotranspiration	Increased Water Proofing
Decreased Turbulent Transport	Reduction of Wind Speed

1.3 Heat Waves in Pakistan

In Pakistan, heat waves frequency has increased as a result of climate change [11]. Pakistan observes variety and diversity in its geographical and climatic patterns. From high mountains to the Indus plains in the country, there are wide variations in the conditions of the country. The heatwave event of 17-24 June, 2015 had caused a significant impact on the people with a death toll of 1200. Temperature recorded was highest since 1979. In the Figure 4, anomalies in temperature and humidity for the period of 1961-2007 are presented. It shows that 6.2% increase in relative humidity is observed whereas temperature increased is 0.25 °C in 46 years.

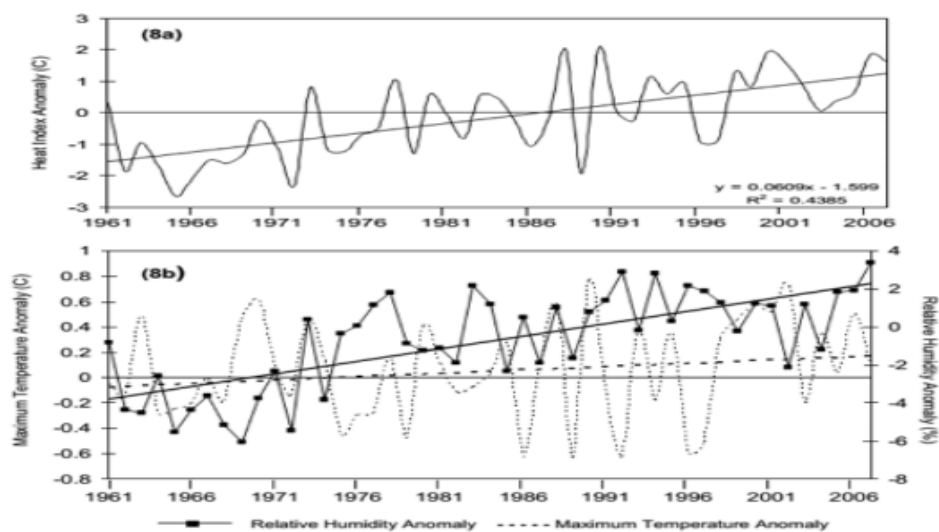


Figure 4: a) Heat Index Anomalies in Pakistan b) Maximum Temperature and Relative humidity Anomalies for the Period 1961-2007 [12]

Karachi was the most affected city with the greatest number of casualties and highest temperature of 49 °C was recorded in Larakana, Sibi and Turbat. This city was affected the most due to number of reasons which are rapid urbanization, population growth, industrial activities and anthropogenic heat dissipation. The city hosts more than 20 million population with a density of 4115 persons per square kilometer. UHI effect is very significant in the major portions of cities like I I Chundrigar Road, Gulistan-e-Johar and commercial areas in Defense Housing Authority Schemes. UHI is a major health risk in Karachi, creating thermal discomfort with people walking around. Tall buildings, slow process of evapotranspiration, waste heat from automobiles and urban canyon effect all contribute to the micro-climate change of the area. Mean maximum temperature (MMxT), mean minimum temperature(MMiT) and mean annual temperature (MAT) from 1976 to 2005 (31 years) is observed to be 2.7 °C, 1.2 °C and 1.95 °C respectively [13]. Karachi Heat Index is shown in the figure below for the heatwave period.

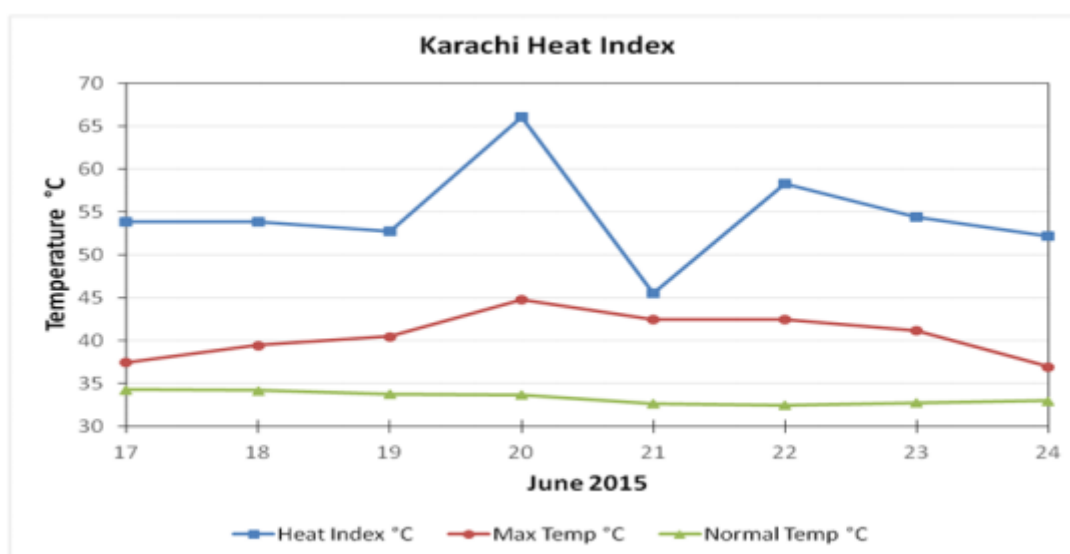


Figure 5: Karachi Heat Index from 17 to 24th June,2015 [14]

1.4 Description of Microclimate

There are number of Urban microclimates in Karachi but the one with significant UHI effect is I I Chundrigar Road with number of tall buildings, offices and residential complexes. The average surface temperature of the region within the city is from 45° to 50°

C during the high heatwave events. High surface temperatures result in the thermal discomfort caused by the convective heat transfer. So, to evade the harmful consequences, some mitigation measures like using high-albedo materials for pavements, reflective coatings and change in the building material are proposed to be implemented.

The objective of this study is to simulate the urban microclimate of the city during a heatwave period in specific part of the Karachi utilizing computational simulation. The situation of 17th to 22nd June is simulated by applying same wind velocity, temperature and solar load to the area by longitude and latitude. Wind Velocities and temperature by hour are obtained from the Pakistan Meteorological department.



Figure 6: Urban Microclimate, Karachi Aerial View [15]

The simulations include wind flow and heat transfer by conduction, convection and radiation. The resulting surface temperatures are validated using experimental data from weather station during the heat wave of Karachi which resulted in number of deaths, increasing human morbidity and mortality.

1.5 Research Methodology

The objectives of this study on the urban microclimate simulation is to develop a 3D Model of the study area and simulate it. In order to perform this, there are some prerequisites which is to apply wind flow and solar conditions on the region and extract surface temperatures and to investigate the heat-wave scenario of urban microclimate, Karachi. Finally, simulation of the effect of albedo on the thermal conditions in the microclimate is conducted.

In order to meet these aims and objectives, the study constitutes of three main sections with further portions. The process is to do literature study on UHI Effect, mitigation measures and CFD rules and guidelines. After getting acquainted with the literature, CFD simulation is performed with all required data and conclusion is made.

The initial phase involves the literature study from which input and target variables are evaluated. All the data to be required in this simulation will be gathered and assembled for modelling and theory. Study area is analyzed with all the conditions affecting it such as solar and wind flow conditions. Mitigation measures of changing albedo values and its applications are studied.

Satellite Data is used to compare the surface temperature contours obtained from the CFD study. In the CFD Study, computational domain, wind flow and solar load are modelled. To validate the results we obtained, there are two validation studies conducted to validate the surface temperature and wind flow. After the simulation of more than 20 cases of the microclimate, the worst-case scenario is selected and mitigation measure of increased Albedo is applied at different surfaces such as concrete, pavements, buildings etc. Improved case and the normal case are compared and results are discussed.

Finally, in the conclusion phase, the data from normal case and the mitigated case is used for comparison. This comparison is based on the surface temperature obtained on the 15 points of the study area. Comparison is made among normal case, reflective building, reflective concrete and coatings. Future recommendations are made for future researchers.

2. Literature Review

Nowadays urban microclimate is studied in two different approaches 1) Observational Approach 2) Numerical Approach. Observational Approaches refer to field measurements and thermal remote sensing. Second one uses computational power and reduces man hours. Experimental results validate the results produced by CFD simulation. It can solve complex and intricate shapes and designs. It varies from building to global scale and can provide a complete picture of urban microclimate. Such techniques will play an essential role not only in applied studies but also in guiding the improvement of simpler models. Literature provides an insight about urban microclimate as this is the field which requires former results to validate CFD results and simulation. Information is also used from Best Practice Guidelines for CFD [16].

There are numerous kinds of CFD models being used for the simulating urban microclimate. Microscale meteorological models are generally known as CFD models. Input and boundary conditions can be sued from the mesoscale. Turbulence model parameterized and it depends on the CFD model: LES, hybrid URANS/LES, URANS or steady RANS. [17] A review research was conducted in which CFD analysis was made on urban climate. The authors mentioned that urban microclimate can affect the natural parameters i.e. heat transfer, wind flow and solar energy etc [18].

As technology is emerging, countable problems in the climate change have been noticed. It was also observed that urban climate change has severe effects and causes. On the other hand, there are measures as well for curbing this cause. Nurruzman reported few measures to mitigate the causes of UHI effect [7]. He observed and researched that albedo pavement, greenhouse effect and shade trees with proper vegetation can be useful measures to mitigate this effect. Plantation has good efficacy and is an effective method for changing and decreasing the UHI effect.

It has been observed from the past researches that urban climate can change the wind flow as well. There are number of studies conducted on the pedestrian level around building of two meters height. Now a days, the construction of building is not only limited to the indoor environment but the level of pedestrian as well for the outdoor environment. After having a deep analysis of the past researches, it was noted that there is dire need of predicting and homogenizing the wind flow. Lots of numerical simulation was taken place and after so

many trials it was concluded that RANS is cost effective and does not need much computing efficiency [19].

A research conducted on the pedestrian wind comfort around the high rise building with the usage of CFD simulation. It was stated in the research that high rise building is the key issue of wind discomfort. Therefore, 3D RANS model with $k-\epsilon$ turbulence was used to overcome this fact. For the remedial purposes, different canopies were made installed near the south-southwest and east-southwest of the building. The simulations are then compared with the on-site measurements for gaining the best results purposes [20].

Toparlar et. al published a case study on Bergpolder, Rotterdam Zuid Region in which a real urban area is considered and enclosed in circular domain of 1200 m which is further surrounded by hexagonal domain of 2400 m (maximum distance). Boundary conditions are applied on the faces of hexagon and appropriate roughness functions are applied. This study provides a detailed methodology for conducting a CFD simulation on an area of radius less than 10 km (microscale). 3D unsteady Reynolds-averaged Navier-Stokes simulations with the $k-\epsilon$ turbulence model are performed on a computational grid. In this research, realizable $k-\epsilon$ model has been employed to simulate the urban microclimate. CFD simulation can be performed reasonably well for prediction the heat wave and the urban temperature. On a high-resolution grid, 3D URANS model was chosen to increase the climate resilience. From the experimental data, it was observed that prediction has 7.9 percent deviation from the CFD simulation. It was noted that CFD has huge potential to predict the urban micro climate [21].

Sen et. al studied the Power Ranch Community of Glibert, Arizona in the Phoenix Metropolitan Area, an area which experiences severe summers. With the mobile field data measurer, warmest hour was recorded with temperature of 42 °C and a very low wind speed of 0.45 m/s which is a cause of low turbulent transport and increased thermal discomfort. In this study, five scenarios were considered with different albedo values and computational fluid simulation was conducted to check the effect of each case. The materials used were new asphalt concrete, normal concrete, reflective concrete and a reflective coating. Same approach is used in this study and simulation is run. Due to these modifications in the structures around or over the buildings, temperature decreased upto 0.8-1.0 °C. [22].

Based on the orthophotos and LiDAR, a shading algorithm is used in the study of Rose & Levinson [23] in which it was examined how tree shading alters the value of albedo

throughout the year. In another publication [24], thermal conditions were improved using the 4500 m² of reflective pavements in an urban park of Athens. Using the high albedo pavements have been the most effective method in minimizing the UHI effect. It was estimated that peak temperature was decreased by about 2.0 K in a typical summer day.

Janssen et. al studied the wind comfort around the high-rise complex of buildings. The computational grid is modeled explicitly ignoring the minute details on the buildings. The CFD simulation data and the on-field measurement at three positions in the urban canyon are compared and results are deduced [20]. Firdaus et. al adopted the Heroit-Watt Univeristy Dubai Campus as a study area. The study of this particular urban microclimate uses CFD to simulate temperature and wind flow parameters at different pinned locations. As in the previous studies, field measurements were taken to compare with the results of simulation which showed temperature increase of 2.7 °C in the zone 1 and 3 [25]. Setia et al. used ANSYS FLUENT as a CFD tool, taking Madinah as a study area to analyze the thermal comfort, wind velocity and air temperature [26].

A CFD study in the city of Tianjin city used the input conditions from the meteorological station to simulate the effect of wind distribution. Full 3D model of city was developed in this and RANS equations were solved to simulate the urban wind flows and effect of air and surface temperature was recorded. Full-scale model was compared with the micro-scale local model and results produced were similar [27].

Vegetation and plantation play an important role in minimization of UHI effect in urban canopies. Not only this, air and water purification can take place due to green spaces [28]. Urban greening is being increased in number of countries to implement sustainability [23]. Trees and Plantation increases the solar reflectance and alters the insolation (solar radiation) at the ground level. During the development of the urban greening policies, trees and plantation must be considered because of the importance of the albedo of trees and plants.

After studying several models in number of studies for simulating and mitigating the UHI effect, it was observed that validation is very critical for the simulation which is not performed in all studies. RANS and LES were highly used and approached models for balancing the climate resilience analysis. RANS was cost effective and LES was accurate among all models but it is very expensive computationally. All studies are summarized in the Table 2.

Table 2: Previous Studies Review

Title	Location	Model	Limitation	Reference
A review on the CFD analysis of Urban Climate.	Generic	Generic	Few parameters are bit defined i.e. pedestrian wind comfort and thermal comfort.	[18]
A review on the study of urban wind at the pedestrian level around the globe.	Generic	Reynolds Average Navier Stokes (RANS)	None	[19]
Urban Heat Island: Causes, effects and mitigation measures-A review	Generic	Generic	Albedo pavements should be the last option.	[7]
CFD simulation and validation of urban microclimate: A case study for Bergpolder Zuid, Rotterdam.	Bergpolder Zuid Region in Rotterdam, Netherlands	Unsteady Reynolds Average Navier Stokes (URANS)	None	[19]
CFD Modeling as a tool for assessing outdoor thermal comfort conditions in urban settings in Hot arid climates	Madina, Saudi Arabia.	Average Navier Stokes (RANS)	None	[26]
CFD for urban physics: Importance, scales, Possibilities, limitations and ten	Generic	Reynolds Average Navier Stokes (RANS) and Large Eddy Simulation (LES)	Adverse Climate Change	[17]

tips and tricks towards accurate and reliable simulations.				
Steady state CFD modeling and experimental analysis of the local microclimate in Dubai (UAE).	Dubai, UAE.	Reynolds Average Navier Stokes (RANS)	Intermittency of wind flow and surface temperature.	[25]
CFD simulation of outdoor ventilation of generic urban configurations with different urban densities and equal and unequal street widths.	Generic	RANS	Limitations of RANS	[29]
Numerical study of urban canyon microclimate related to geometrical parameters.	Generic	RANS using k-ε model	Limited effect of buoyancy	[30]
Fluid dynamic and heat transfer parameters in an urban canyon.	Generic (two building blocks).	RANS using k-ε turbulence model	Non-stationary behavior of solar radiance and irradiance.	[31]
Use of CFD simulations to improve the pedestrian wind comfort around a high rise building in complex urban area	Dutch City, Eindhoven.	3D Steady Reynolds Average Navier Stokes (RANS)	Wind nuisance problem.	[20]

Numerical simulation of atmospheric pollutant dispersion in an urban street canyon: Comparison between RANS and LES.	Generic (Urban Street)	RANS, RSM and LES	Intermittent and unsteady nature of filed flow.	[32]
CFD simulations of wind distribution in an urban community with full-scale geometrical model	Tianjin City, China	Reynolds Average Navier Stokes (RANS)	Intermittent nature of wind.	[27]
Cool Pavement Strategies for Urban Heat Island Mitigation	Suburban Phoenix, Arizona	RANS / Field Measurements	Only for particular land cover type	[22]
Using Cool Paving Materials to improve microclimate of urban areas	Flisvos Park in Athens Area	RANS / Field Measurements	Boundary Conditions differ considerably in two monitoring campaigns	[24]
Analysis of the effect of vegetation on albedo in residential areas	Suburban Sacramento and Los Angeles, CA	GIS	Shaded areas may be slightly underestimated	[23]

3. Numerical Methods

In this part of the study, the CFD simulation settings and parameters are described. There are two simulations performed, one is main simulation of the 3D urban model and other is for generic two building model for the validation of the computational setup.

3.1 Methodology

This section describes the computational setup. First, target variables to be researched in this study are chosen and then the governing methods are specified.

3.1.1 Target Variables

The main target variable is temperature which is used in the heat wave. There are two main temperature values used for the computational analysis. First, is the surface temperature of the canyons within the circular domain and secondly the air temperature at pedestrian height (2.0 m). The other parameters affecting the results are building locations, building heights, shadowing due to sun direction vector, courtyards, material specifications such as brick and earth. Absorptivity study is performed in which the absorptivity of the area under consideration is decreased to a certain value in order to account for the effect of light-coloring of roads, roofs and facades. After the implementation, a comparison of air temperature at pedestrian height and surface temperature can be made based on the normal situation and the situation with the absorptivity reduction.

3.1.2 Models for Computation

The 3D URANS model is solved with the realizable $k-\varepsilon$ model is used for microclimate [21]. P-1 Radiation model is used [33] for the solar radiation. In this study the realizable $k-\varepsilon$ turbulence model is used as it is very efficient in terms of time and computational cost. Computation is performed according to the best practice guidelines published by [34], [35], and [36]. This computation is based on the ground level temperature which eliminates the effect of transverse mixing which is overestimated by $k-\varepsilon$ turbulence model.

3.2 Geometry

In this section, the geometry of the real microclimate of an area in Karachi, Pakistan with hexagonal domain is described along with the geometry of generic urban buildings for the validation of wind flow. Apart from the Wind flow, ground surface temperature is validated

using Satellite MODIS Product. After the modelling of the 3D real urban area, model in IGES format is exported to the Pointwise where mesh is created using the guidelines discussed above.

3.2.1 Domain of Generic Urban Area

This validation model for the wind velocity considers the flow around a single building of which geometric model is shown in Figure 7. This model has a passage made in the center of the building at the pedestrian level. This configuration was selected as real-time wind tunnel measurements for this model [37]. Similar study was performed with different approach by [38], in this study velocity and turbulent kinetic energy (TKE) profiles are compared.

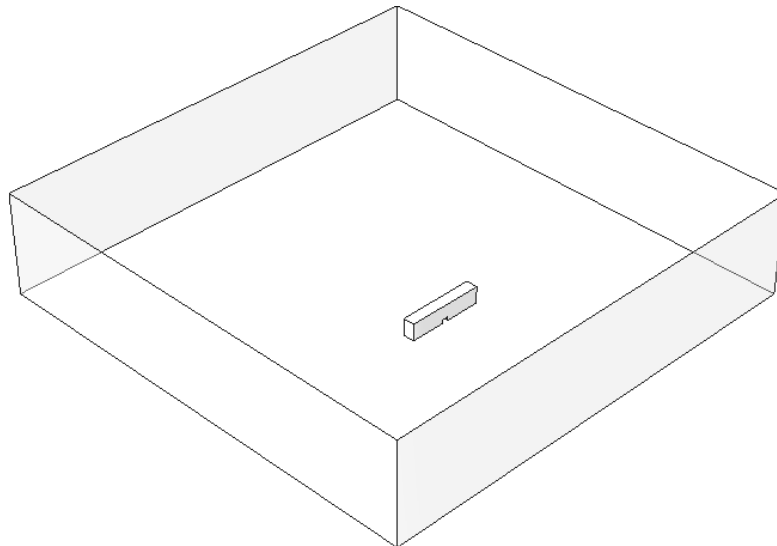


Figure 7: Single Building Model with a Passage

The model of our simulation has a height of 108m and a width of 480m, which indicates a blocking ratio of 2.8% according to the [39]. The shape of the section of the simulation volume is equivalent to the building facade exposed to the wind. The depth of our simulation volume measure 480m, of which 180m are located before the building. The mesh show in the Figure 8 and Figure 9, has 12,645,371 cells and 2,359,109 points. It contains 12,339,865 tetrahedral and 305,506 pyramids.

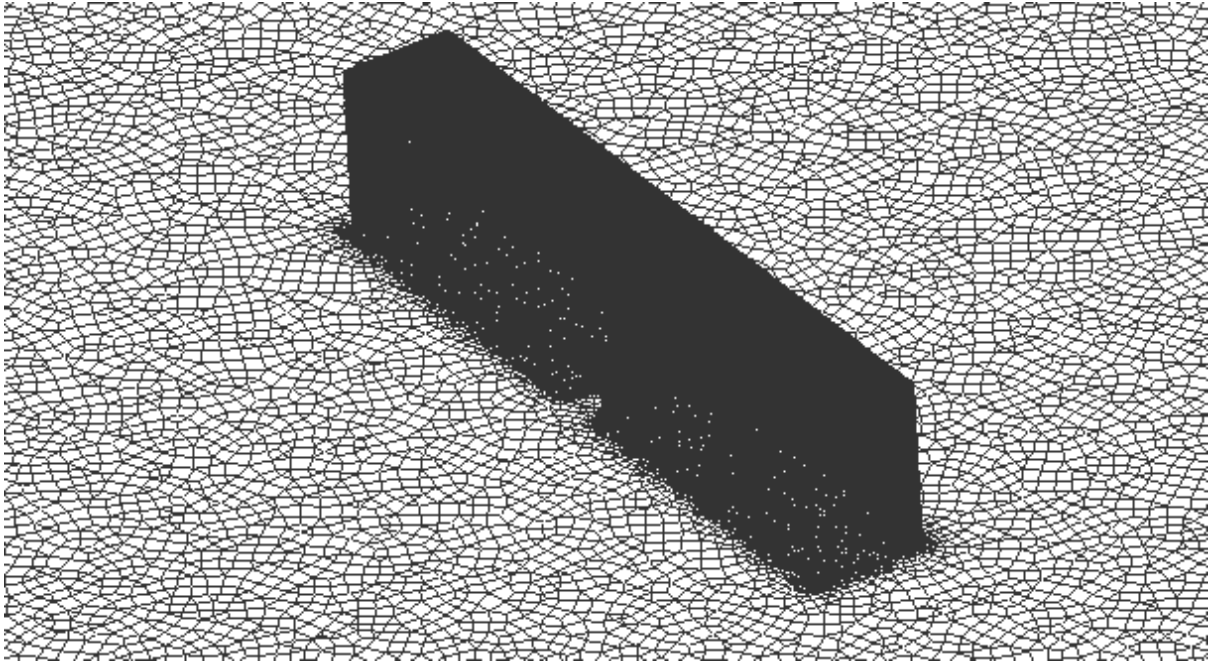


Figure 8: Computational Grid of Single Building with the Passage (PointWise)

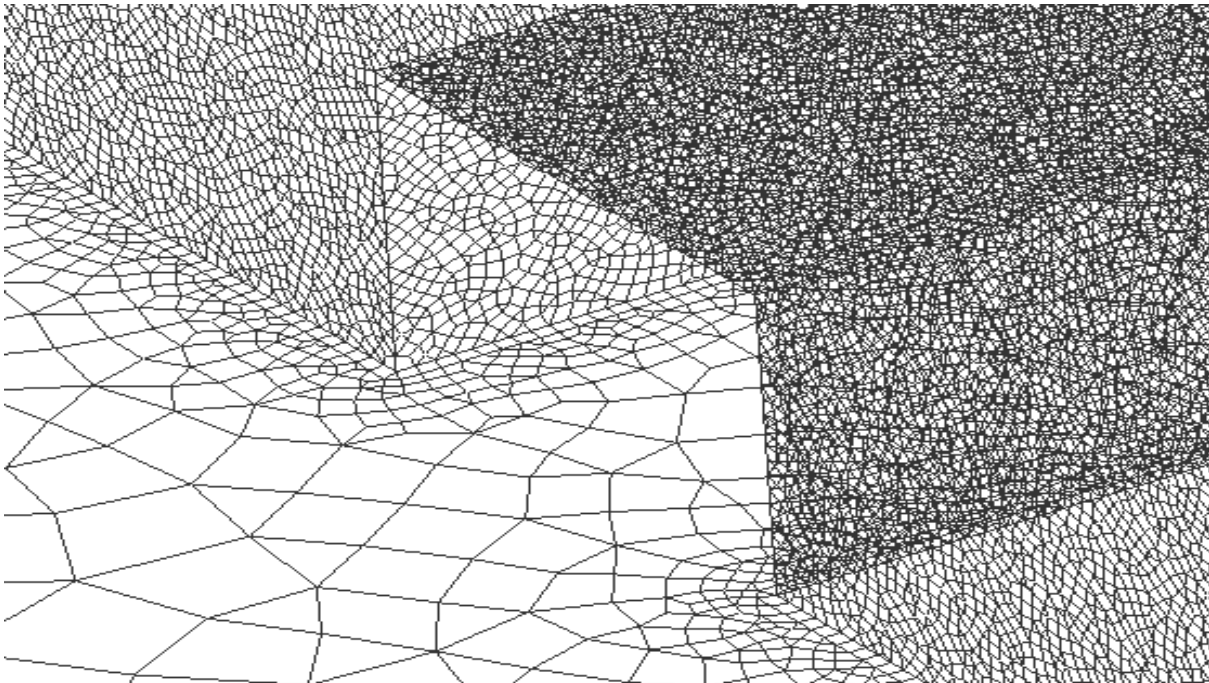


Figure 9: Computational Grid of Passage in a Single Building

3.2.2 Domain of Real Urban Area

In this study, the domain's highest building has a height of 50 m. The computational domain is shown in Figure 10. The aerial view of the real domain with the surroundings is shown in Figure 11. The height of the domain is 400 m as it is recommended in all the guidelines referred. $8H$ is the distance from the ground to the pressure-far field in the domain which is greater than

the threshold $5H$. This also meets the condition of the blockage ratio and lateral distance. Longer distances from the circular domain to the inlets and outlets is highly recommended which means fully developed flow when it enters the urban island.

The computational domain in this study is hexagonal and contains a circular sub domain with urban part as discussed that includes all the buildings of the region. Each edge of the hexagon measures 692 m yielding maximum distance of 1200 m inside the domain. Circular domain has diameter of 600 m. The buildings inside the subdomain are modeled with general details of volume, intricate details like windows, doors, extensions or designs are ignored as they do not have major effect on the heat transfer analysis. Considering the positioning and dimensioning of the region, the blockage ratio of maximum 3% is satisfied.

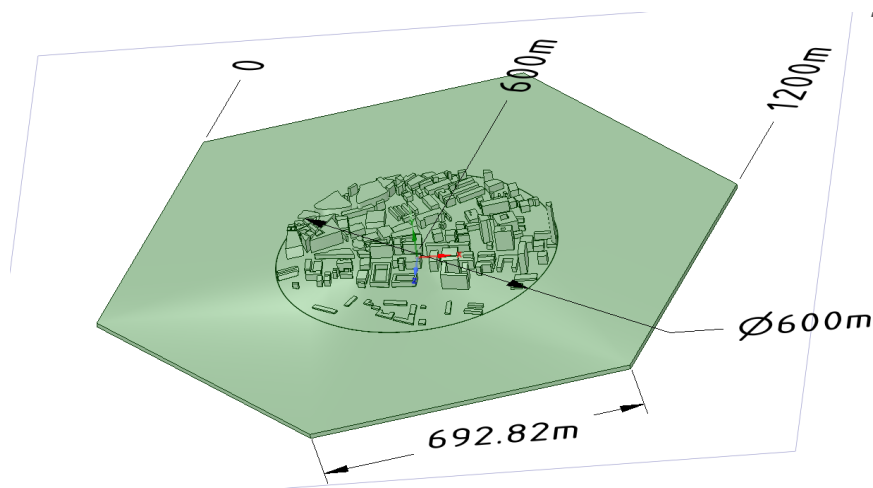


Figure 10: Computational Domain of Real Urban Area

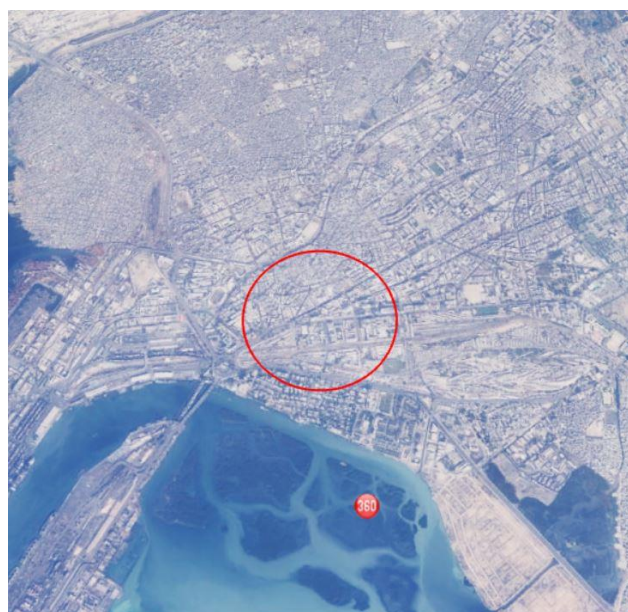


Figure 11: Satellite Image of the Urban Area Domain

3.2.2 Computational Grid

For the CFD simulation, meshing is very important aspect to produce reasonable results. Ground plane model of the computational grid is shown in Figure 12. Computational Grid as shown in Figure 13 of the model is created in PointWise [40] using T-Rex command. A SpaceClaim (ANSYS v17.2) model is converted into an IGES format which is suitable for PointWise. The file format is called Initial Graphics Exchange Specification (IGES) and this format allows PointWise to load the drawing successfully. The 3D Model after getting exported to PointWise is in the form of database which will be converted into the connectors. Connectors will be dimensioned according to the guidelines provided. Mesh will be finer near the ground, area of the interest but as the distance from the target area increases, the mesh becomes coarser. Total number of cells are 52, 312, 459 including 50,798,172 tets and 1,514,287 pyramids as seen in Table 3. Spacing between the cells in the circular subdomain is kept 0.3 m, spacing in the boundary of the circular domain is 2 m, as the distance from the center increases, cell spacing increases with 7 m at the boundary of the hexagonal domain.

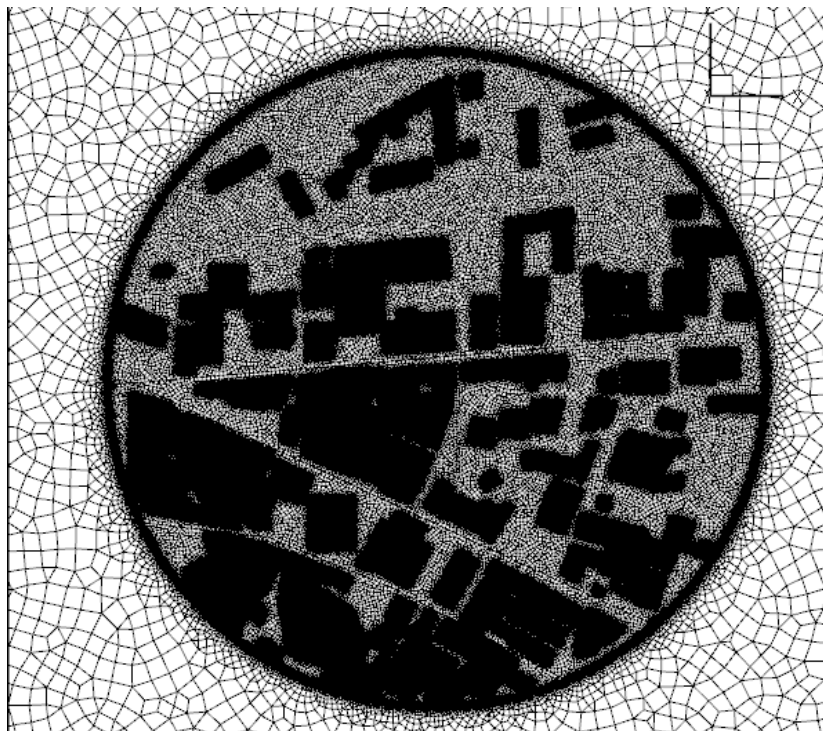


Figure 12: Ground Plane Model of Urban Microclimate, Karachi

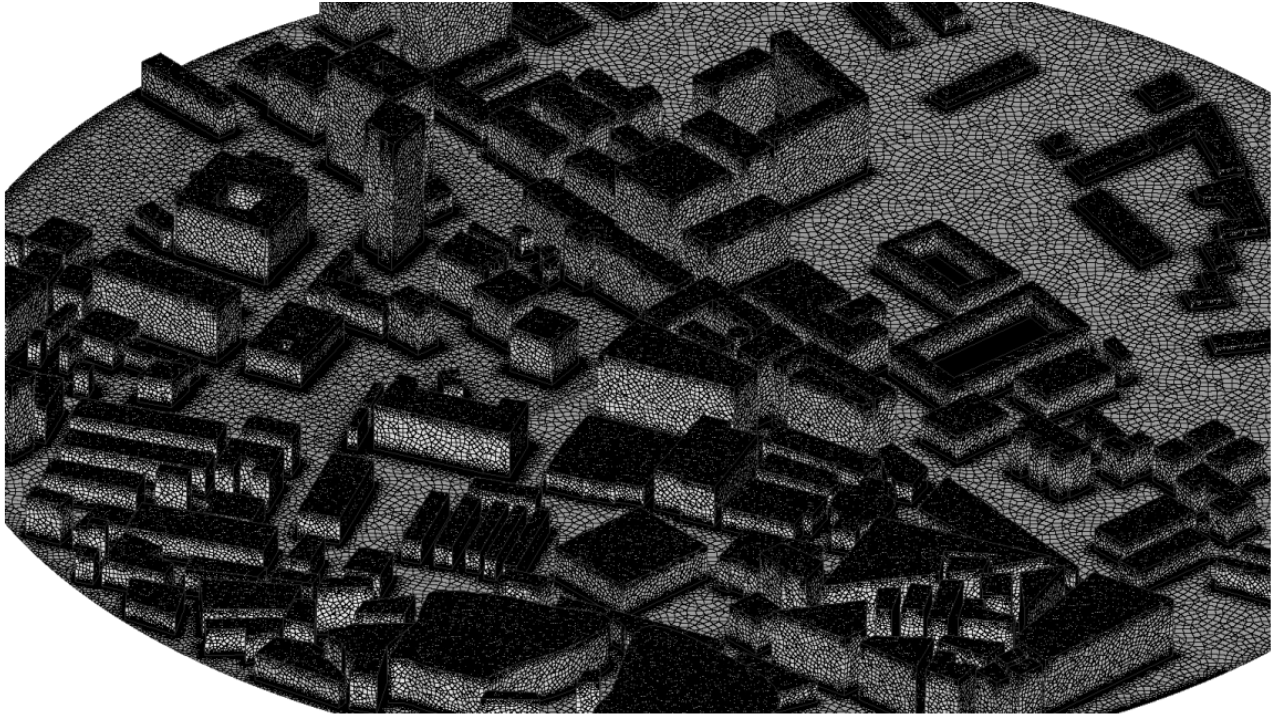


Figure 13: Circular Sub domain in Computational Grid

Table 3: Cells count of Computational Grid

Cells	
Type	Count
Tets	50,798,172
Pyramids	1,514,287
Prisms	0
Hexes	0
All	52,312,459

After completing the domains of buildings walls, circular domain ground, hexagonal domain ground, sky and inlets/outlets, all domains are converted into one block. Block is initialized to form a volumetric domain. Boundary Types are selected in the PointWise and further settings will be done in ANSYS Fluent v17.2. In the Figure 16, urban microclimate is depicted with a real Google Earth Image which is modeled for the CFD study.

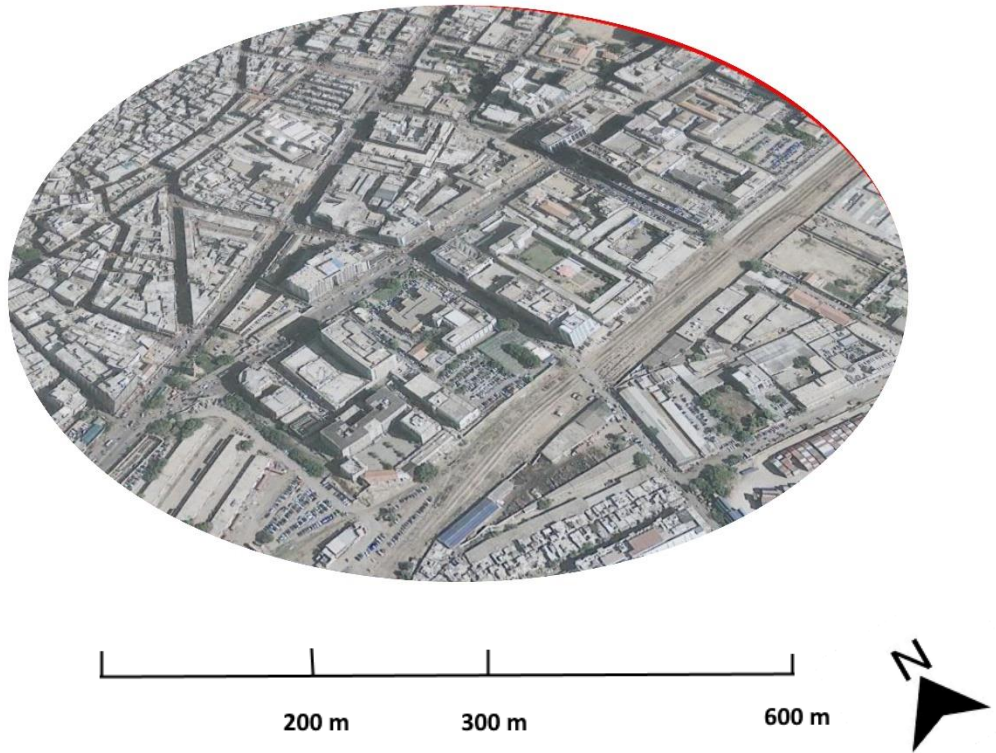


Figure 14: Real Urban Domain under study

3.3 Initial and Boundary Conditions

In this part of the study, the initial and boundary conditions of the CFD simulation are presented. This includes wind velocity, aerodynamic roughness, solar radiation, energy equation, Viscosity model and many other settings.

3.3.1 Boundary Conditions

First is the velocity inlet conditions for each case described. The velocity inlet is the boundary from where the windflow enters the computational domain. Velocity is given constant [41], input wind velocity is provided by the meteorological department of the Karachi. Velocity vector is always normal to the boundary. Apart from the velocity magnitude, turbulence intensity of 10% is prescribed [31]. Moreover, the temperature of the velocity inlet (wind flow) will be specified in the “Thermal” portion of the velocity inlet boundary condition. Temperature of the inlet is provided by the data provided by Meteorological Department.

The circular ground, hexagonal ground plane and the building walls are defined as the wall boundaries. Wall boundaries can be defined with the roughness height, roughness constant, thermal conditions and radiation conditions. For the building walls, the roughness height is assumed zero and roughness constant of 0.5. For circular ground plane in which there are streets, courtyards and other obstacles, roughness is calculated from the following relation [35]:

$$k_s = 9.793 \frac{z_o}{C_s}$$

‘ z_o ’ can be selected on the basis of surroundings which is further explained in the next section.

In the geometrical model, each region in the hexagonal domain and circular subdomain is given a sand grain roughness. According to the first cell of the height, roughness height is adjusted to validate the formula. The thermal settings for the ground walls in the circular subdomain and hexagonal domain are same.

3.3.2 Aerodynamic Roughness Length

For this simulation, velocity profile is constant which is developed once enters the real urban area to be simulated is approached. The inlet profiles of wind velocity, turbulent kinetic energy and the turbulent dissipation rate are linked to the aerodynamic roughness length (z_o) of the terrain, upstream of the computational domain. These values are obtained from Davenport classification by [42] . In the Figure 17 shown below, there are suggested values of (z_o) for our real urban area. The roughness values are assigned for each 22.5° intervals. For each of the inlet or outlet is assigned a (z_o) value.

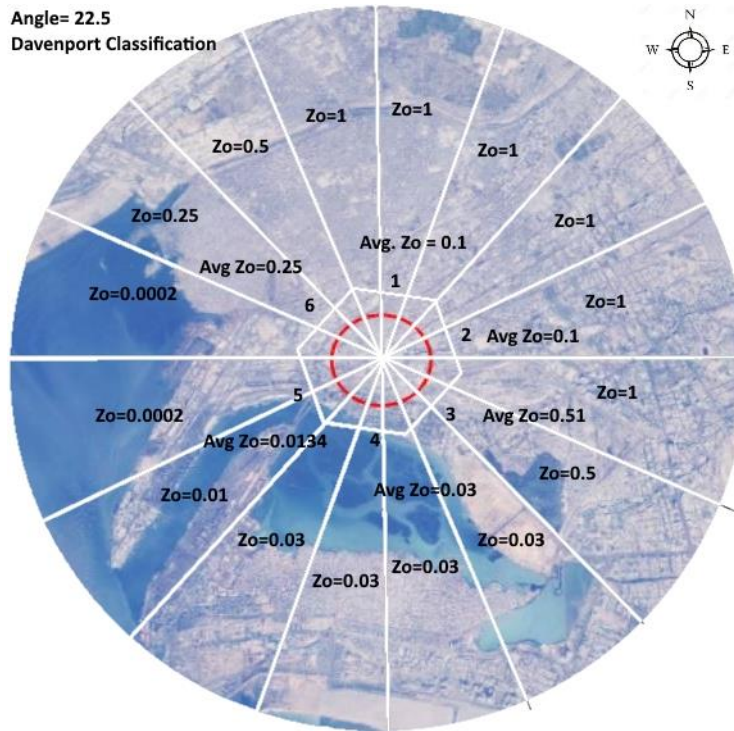


Figure 15: Estimated Aerodynamic Roughness Length. Red line Circle is the subdomain and white hexagon is the complete computational domain. Aerodynamic Roughness Length are given according to Davenport Classification

3.4 Solution Methods and Controls

Solution Parameters are used to indicate the methods to be used for solving the differential equations. Numerical approximations and iterative convergence criteria set in this computation are described.

3.4.1 Numerical Approximations

A second order numerical scheme and SIMPLEC algorithm is used for the simulation.

3.5 Thermal Model

In order to consider the effect of solar load and radiation on the real urban area, a solar radiation effect should be modelled. A model with radiation and convection must be considered to take in account this effect. Gravitational Acceleration is defined for y-axis as -9.81 m/s^2 . For solar model, P1 radiation model is selected [33]. In the Solar Load settings, solar calculator is configured according to the mesh orientation and real urban area coordinates for sun direction vector. The necessary inputs for longitude and latitude are 67 and 24.85 respectively which

defines the center of our study area. The time zone of the area is +5 Greenwich Mean Time. After these settings, mesh orientation is defined in the Solar Calculator. Sun direction vector is calculated automatically by the solar calculator when specific date and time is entered according to the time of heat wave, 2015. After all these settings, direct normal solar irradiation affecting the surface temperatures of the region is calculated. The model is now ready for the surface temperature calculations. All the CFD settings are presented in Table 4.

3.6 Settings Table for Computation

Table 4: CFD Settings

Fluid		Wall Functions	
Air (Incompressible, Viscous)		Standard Wall Functions	
Density	$1.225 \frac{kg}{m^3}$	Von Karman Constant	0.4
Viscosity	$1.7894 * 10^{-5} \frac{kg}{m * s}$	Gravitational Acceleration	-9.81 m/s ²
Geometry		Inlet Boundary Conditions	
Edge Length	692.8 m	Type	Velocity Inlet
Width	1200 m	Velocity Profile	Constant
Length	1200 m	k (Turbulent KE)	10%
Height	400 m	e (Dissipation Rate)	1
Urban Area Diameter	600 m	Outlet Boundary Conditions	
Solver	RANS	Type	Pressure Outlet
Momentum	Second Order Upwind	Radiation Model	
Energy	Second Order Upwind	Type	P1
k-ε model	Second Order Upwind	Solar Load	Solar Ray Tracing
Turbulence Model		Interpolation Scheme	
Realizable k-ε Model		Pressure	Standard

Mesh		Coupling	SIMPLEC
Type	Unstructured	Location (Longitude and Latitude)	
Cells	52,312,459	67.00 and 24.85	

4. Results: CFD Simulation of Microclimate

CFD analysis is performed using specific set of guidelines [33], the boundary conditions which are applied at the inlets are the real boundary conditions obtained from the data provided by Meteorological Department of Pakistan, Weather station which is around 15 km from the our study area. Thus, we have assumed the wind velocity and the air temperature at the meteorological station is not varied that much as wind currents travel to the study area. However, although the outputs are intended to be similar as well, so the data needs to be validated. The surface temperature which are calculated from the CFD simulation are validated from surface temperatures, based on satellite measurements. These measurements are obtained from the MODIS product. Heat wave measurements are reported in a technical report published by Ministry of Climate Change. [14]. The other validation study performed is for the wind velocity profile along the street canyon. [43]

4.1 Validation of Surface Temperatures

The first validation study is related to the surface temperatures of the region under study and the effect of wind flow and solar radiation on surface temperature. The aim of this validation is to compare the real time measurements of surface temperatures in the city of Karachi to the measurements, and the temperatures obtained from a CFD simulation with meteorological inputs.

4.1.1 Satellite Measurements of Surface Temperature

In order to measure the Satellite surface temperatures for specific location (Coordinate Location). HDF file from the online MODIS data base is used and temperature measurements are extracted using Qgis 2.18. Table 5 presents the time, date and product used for the average surface temperature of the region.

Table 5: Table of Data acquisition of Satellite Temperatures

Products	Mod11c1		Myd11c1	
Time	Night	Day	Night	Day
18	17.79999924	6.800000191	22	-
19	18.39999962	5.800000191	-	9
20	17.60000038	6.599999905	21.79999924	9.80000019073486 , 9.60000038146972
21	-	-	-	8.800000191
22	17.20000076	6.400000095	21.60000038	-
23	-	-	-	8.600000381

Products	Mod11b1		Myd11b1	
Time	Night	Day	Night	Day
18	22.20000076	11.19999981	2.400000095	-
19	-	10.19999981	-	13.39999962
20	22	11	-	13.19999981
21	-	-	-	-
22	21.79999924	10.80000019	2	-
23	-	-	-	13

Products	Mod11a1		Myd11a1	
Time	Night	Day	Night	Day
18	22.10000038	11.10000038	2.400000095	-
19	-	10.19999981	-	13.39999962
20	21.89999962	10.89999962	-	-
21	-	-	-	13.19999981
22	21.70000076	10.69999981	-	-
23	-	-	-	13

According to the measurements of Heat Wave of June, 2015, the average surface temperature of the region under study from 18th June to 23rd June is 308.33 K. The considered validation within this study is the observation of June, 2015 surface temperature values using MODIS products. Based on the times selected for data collection, surface temperature values of the urban microclimate are provided in the plot in Figure 18 generated from Table A2.

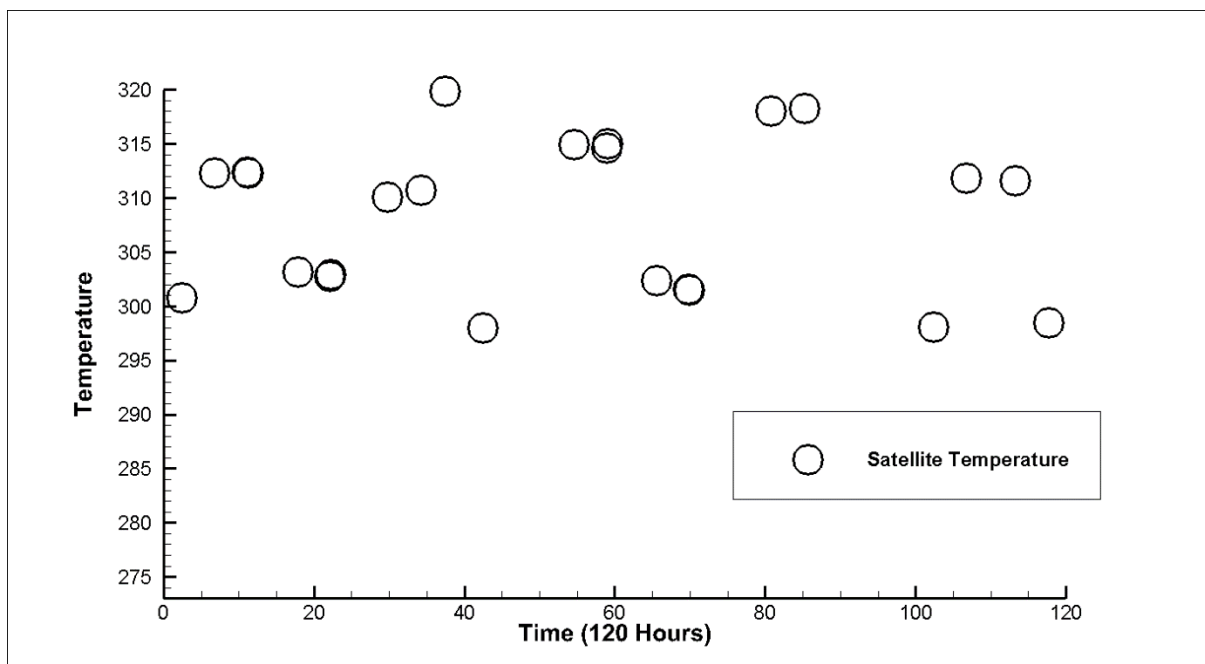


Figure 16: Average Surface Temperature from MODIS Product from 18th June 2015 to 22nd June 2015

The surface temperatures are averaged over the region which means data does not consider any maximum or minimum values.

4.1.2 Validation Study

In order to compare the 3D urban model with the average surface temperature calculated from the MODIS product [44], a model of microclimate is generated. This model is computational model of the area and is subjected to the wind velocity and solar radiation conditions. Time interval of the satellite measurements and the computational simulation is same. 3D modelling phase and the inputs to the domain are presented.

Initial conditions and boundary settings are described in the section (3). For accurate results and ideal simulation, homogenous zone is required at all of the inlet sections.

4.1.2.1 Measured Meteorological Conditions

For the time span of heat wave being simulated, we need meteorological conditions presented in Table 6 are the most important inputs for the simulation in order to validate the CFD measurements at corresponding time periods. The Meteorological department of Karachi has a measurement station at Jinnah International Airport, Karachi. This department provides the values of radiation to the surface to the surface at every hour. This is hourly data in which wind velocity and inlet temperature is specified. From this data, the date and time are used for specifying the sun direction vector in CFD Model. Air Temperature, radiation, wind velocity and wind direction are used directly at the inlets from the database.

Table 6: Input Data for Selected hours from the Meteorological Department of Karachi

Case	Date	Year Day	Time	Temp	Direction	Wind Velocity (knots)	Wind Velocity
1	18/06/2015	168	0400Z	34.5	NW	04	2.05776
2	18/06/2015	168	0900Z	38.0	SW	14	7.20216
3	18/06/2015	168	1200Z	37.5	SW	12	6.17328

4	18/06/2015	168	1400Z	35.0	SW	08	4.11552
5	18/06/2015	168	1600Z	33.5	SW	06	3.08664
6	18/06/2015	168	2200Z	33.0	SW	08	4.11552
7	19/06/2015	169	1000Z	39.5	SW	10	5.1444
8	19/06/2015	169	1300Z	37.5	SW	10	5.1444
9	19/06/2015	169	1600Z	33.5	SW	08	4.11552
10	19/06/2015	169	1800Z	33.0	SW	06	3.08664
11	19/06/2015	169	2200Z	32.0	NW	04	2.05776
12	20/06/2015	170	0300Z	34.0	NW	04	2.05776
13	20/06/2015	170	0900Z	43.5	SW	10	5.1444
14	20/06/2015	170	1600Z	36.0	SW	06	3.08664
15	20/06/2015	170	2100Z	35.0	NE	04	2.05776
16	21/06/2015	171	0200Z	34.0	NE	02	1.02888
17	21/06/2015	171	0900Z	41.5	NE	10	5.1444
18	21/06/2015	171	1500Z	39.0	NE	10	5.1444
19	21/06/2015	171	2100Z	36.0	NW	04	2.05776
20	22/06/2015	172	0100Z	35.0	NE	10	5.1444
21	22/06/2015	172	0700Z	40.0	SE	06	3.08664
22	22/06/2015	172	1300Z	38.0	SW	10	5.1444
23	22/06/2015	172	1700Z	35.5	SW	04	2.05776

With this data, the simulation cases have been modeled separately. Inlets of the hexagonal domain are changed according to the wind direction around the urban subdomain. Wind direction along with the boundary number indicated in Figure 15 is shown in Table 7.

Table 7: Inlet and Outlet Faces and Walls of the Computational Domain at different orientations

Direction	Inlets	Outlets	Walls
SW	1,2	4,5	3,6
W	5,6	2,3	1,4
NE	1,2	4,5	3,6
E	2,3	5,6	1,4
S	3,4,5	1,2,6	

NW	3,4	1,6	2,5
----	-----	-----	-----

4.1.2.2 Validation Study of Wind Flow

This study is based on number of CFD computations to evaluate the wind velocity in the pedestrian path drilled in the single building. Simulation is carried out with the FLUENT software in a similar way as in [43] compared to the results of Wind Tunnel Measurements of [37]. The ratio U/U_0 is plotted against the distance in the passage of building (0-12 m) simulated with different models: $k-\epsilon$ 2nd order, $k-\epsilon$ realizable, RNG and RSM. The results are shown in Figure 19.

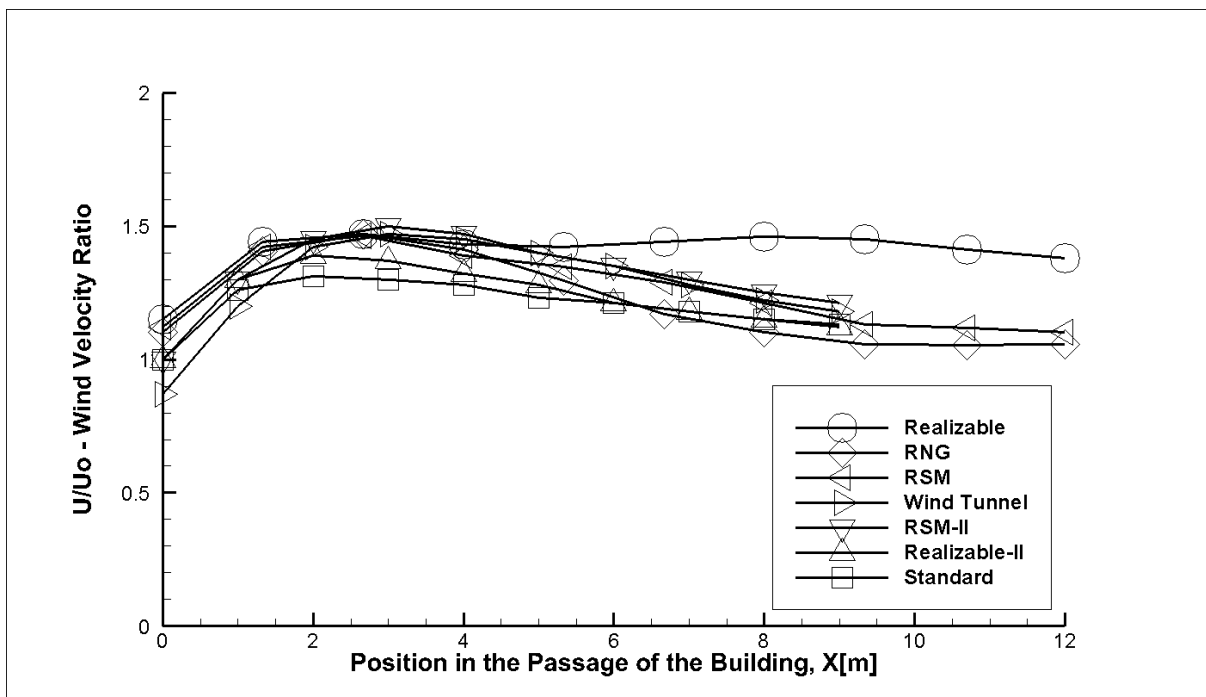


Figure 17: Wind Velocity Ratio vs Position in the Passage of building at different Settings

Above Plot shows the results of validation study performed in our study and [43].

The standard $k-\epsilon$ model provides better result to validate the wind tunnel experiment results presented by line (+) in the Figure 17. Similarly, $k-\epsilon$ realizable model yields better results than

standard model to quantify the discomfort estimation. Still error occurs in both models as compared to the wind tunnel results. The Reynolds stress model provides close results to assess wind comfort in the passage of the building. It determines accurately the position of the maximum discomfort. If a comparison is made among all the models simulated, all models provide accuracy under 15%.

4.1.3 Results and Comparison (Real Urban Area)

There are 23 cases which are simulated. From each of the case, air temperature and surface temperatures are obtained and compared with Satellite temperatures extracted from the MODIS. The temperature measurements are simulated for 15 selected points in the 3D model distributed around the microclimatic region of Karachi seen in the Figure 18.

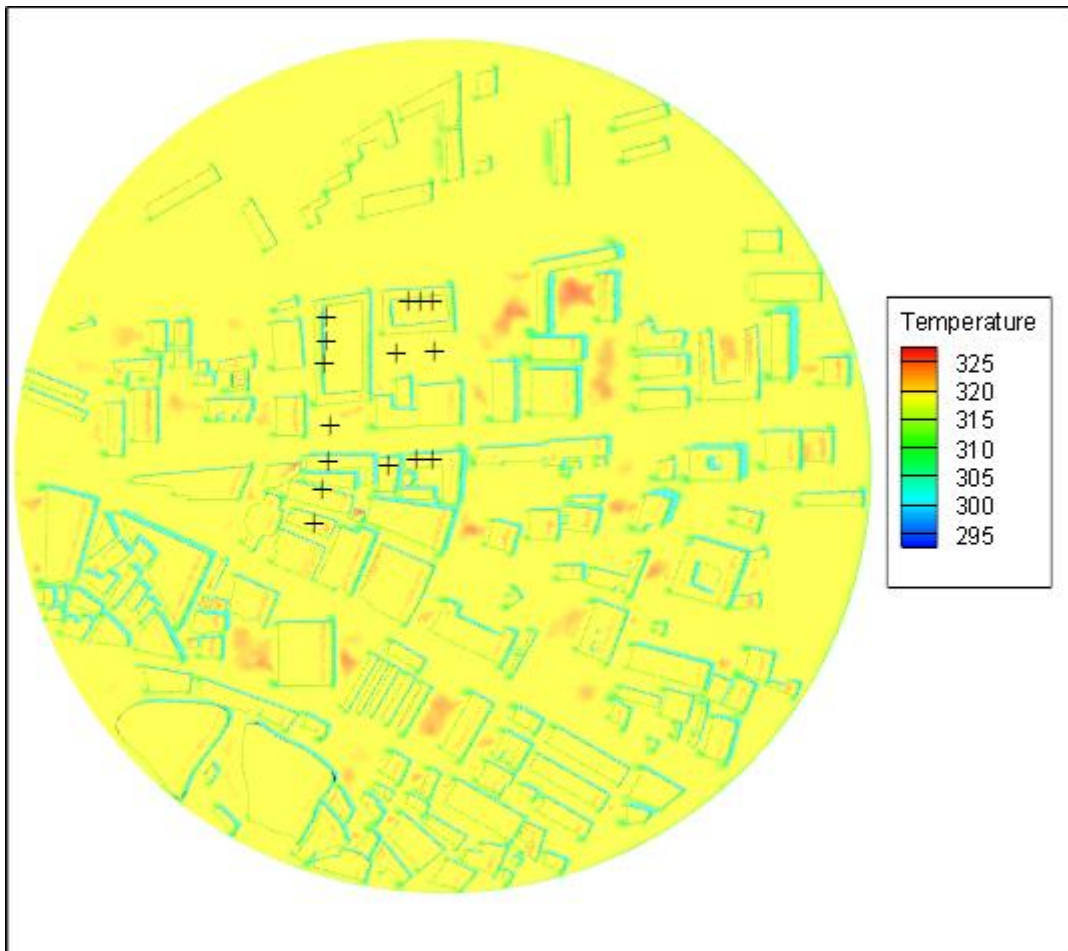


Figure 18:Representation of Microclimate and 15 Data Points with Temperature Contours 19th June 1300

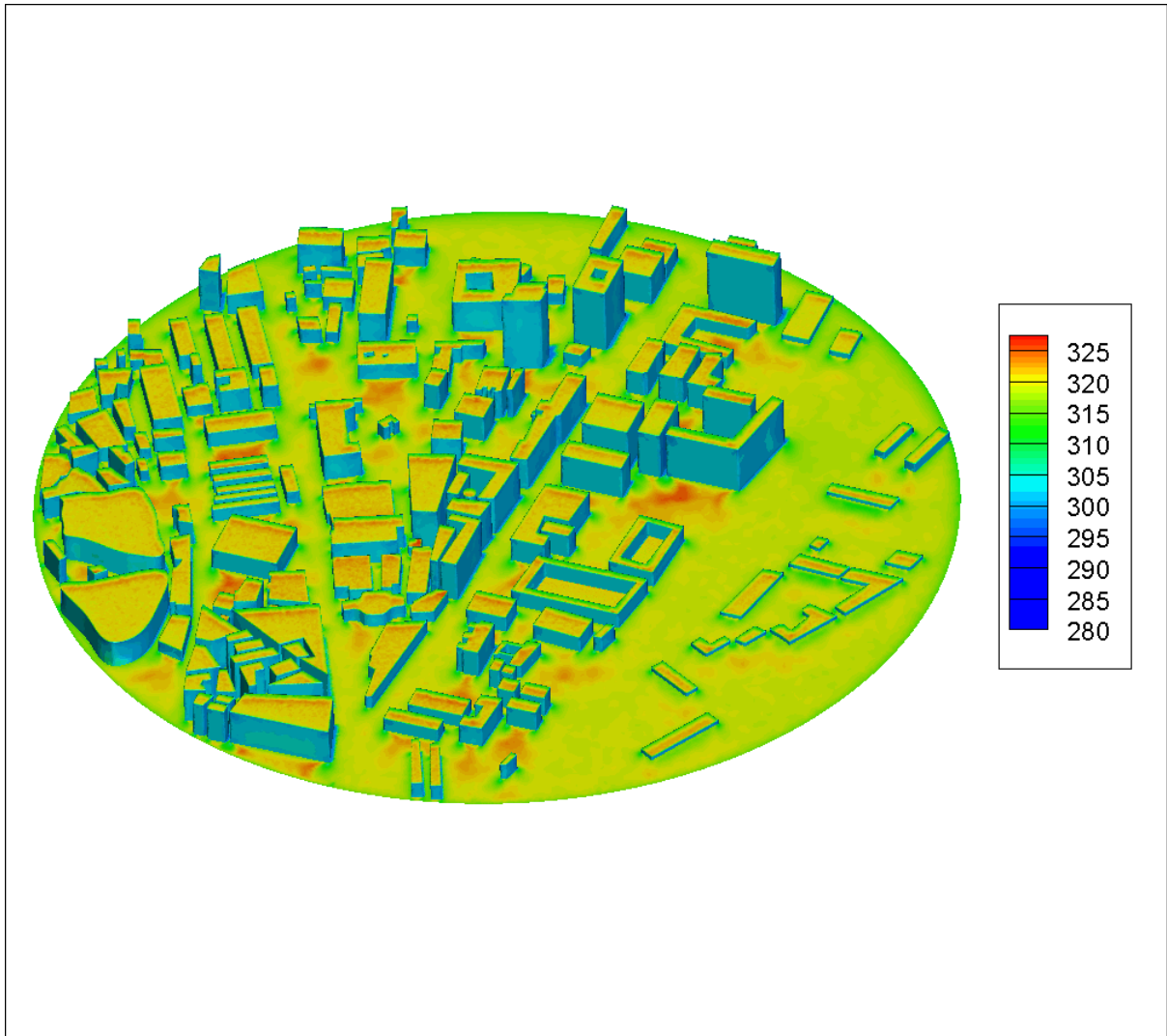


Figure 19: 3D View of an Urban Microclimate Surface Temperature 19th June 1300

The 15 points are randomly selected around the highly affected areas where temperature is higher which ensure that temperature is being measured at core of the circular subdomain. In the end, the 15 surface temperature values are averaged for a single value which are compared as simulated average surface temperature. These Data points are plotted in Figure 20. The comparison between the results from satellite and simulation is shown in Figure 19.

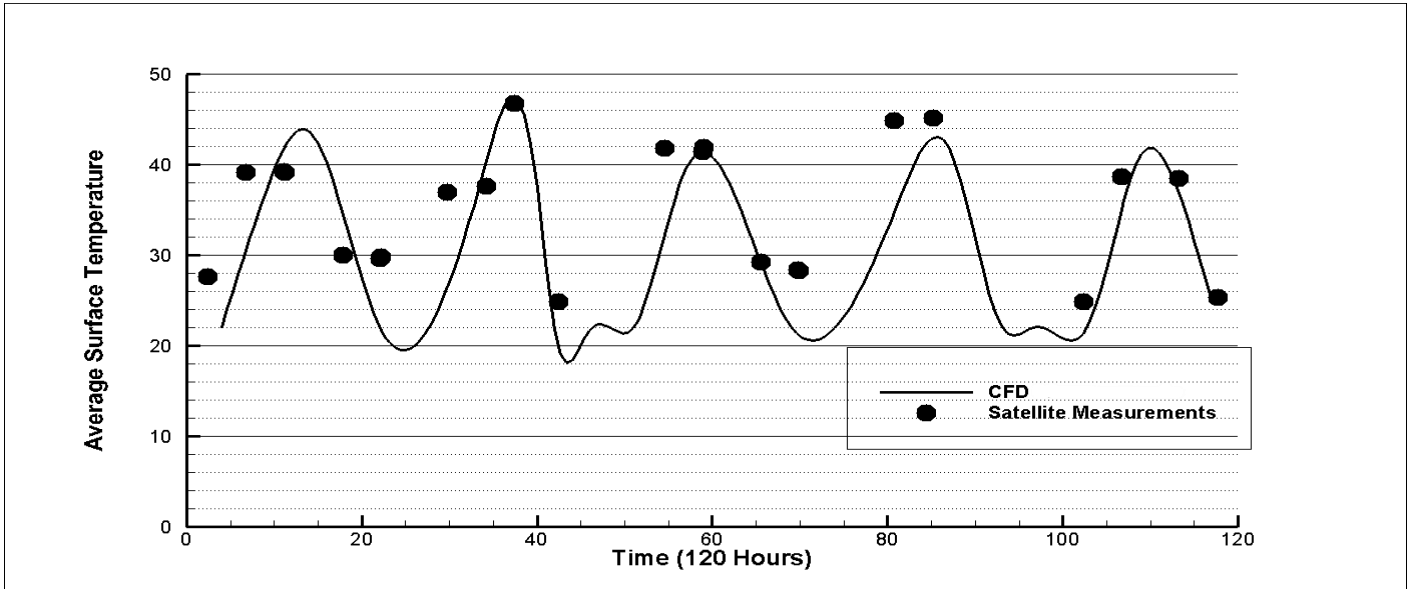


Figure 20: Comparative Graph for the model validation results

The results of the validation are in good agreement with the satellite measurements except the results which are simulated in the night time. This error can be justified due to cloud cover decreasing the accuracy of satellite measurements. Surface temperatures drop usually at the evening time, this is due to the low amount of the radiation after 1700 hours. Sun direction vector angle is low as well. In the starting two days or nearly 40 hours, temperatures are close to those measured from the satellite but after 40 hours from 18th-June, surface temperatures are overestimated by 2 to 3°C. There might be number of reasons for these differences, surface temperature from MODIS are higher due to changing behavior of wind from 20th June till 22nd June, due to which there is a large effect on the output.

In general, computational analysis of real urban area with solar loading showed reasonable results with the real time values. The comparison of the satellite and CFD results shows that computational results are properly validated. In the following section, a mitigation measure is adapted to reduce the street surface temperature.

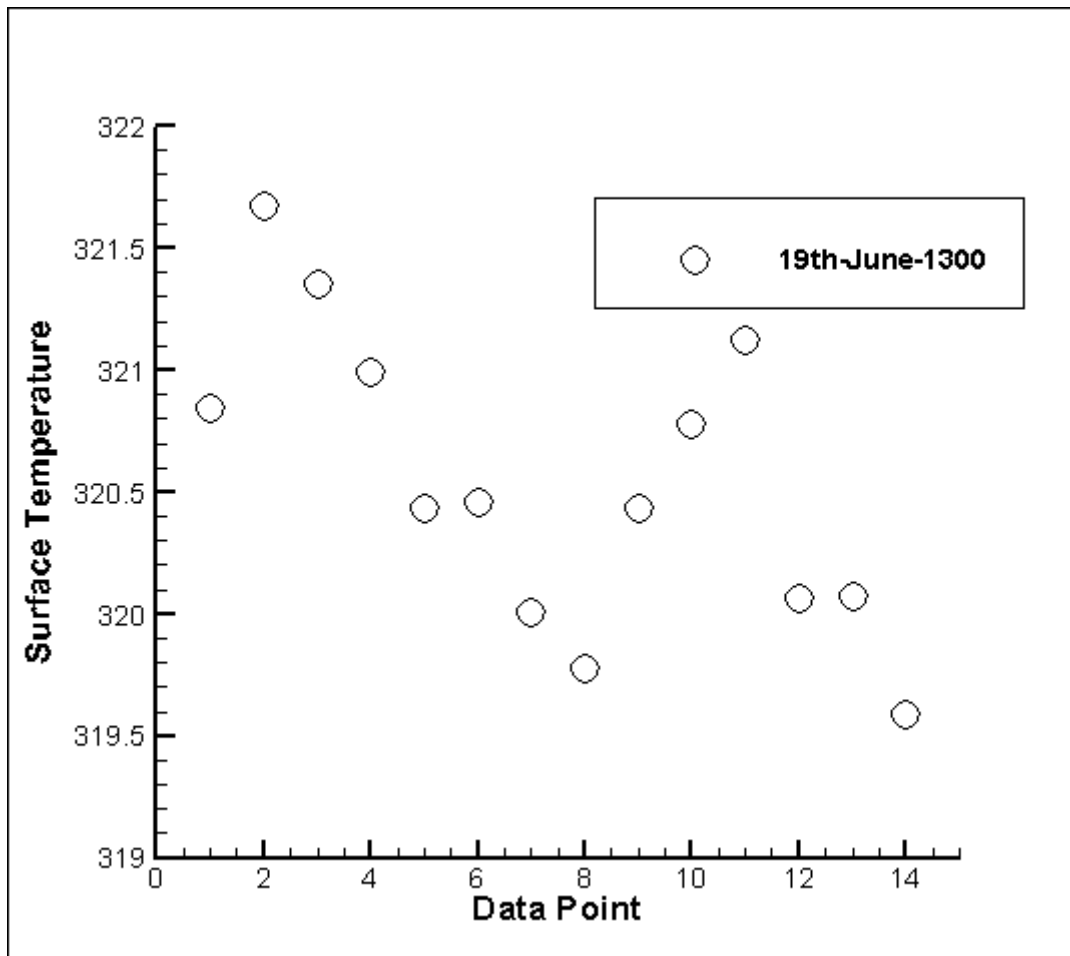


Figure 21: Surface Temperature Distribution based on data points used in validation model. Note that average is calculated as 320.54 K

5. Mitigation Measures

This section deals with the application of materials that can reduce solar absorption and thus create a more comfortable urban microclimate for pedestrians. The aim is to improve the thermal comfort conditions and reduce the intensity of heat. This can be done by taking number of mitigation measures and evaluate the results by computing the temperature difference with the case of 19th-June-1300, on which surface temperatures was almost 47 °C and can be reduced by using cool paving materials [24]. It has been shown that that if stone mastic asphalt is used instead of normal asphalt, thermal conditions are improved. [45]

Urban Heat stress can be reduced by coating or covering the urban landscape of asphalt, brick, metal and other heat absorbing materials. Building's roof is typically black or gray in the urban cities which can be light colored to reflect up to 50% of the light incident on it. Not only have this, light-colored concrete and white roofs reduced the energy demand of a specific building.

Other measures like plants and green roofs can also contribute to reduce the urban heat island effect [46]. Gaining thermal comfort from plants highly depends on the space, time and plant properties. It is not necessary if vegetation can produce desirable results in every orientation [47].

5.1 Cool Pavement Materials

Using conventional asphalt on the pavements adds to the urban heat island effect. A coating material is required to reduce the intensity of heat absorbed. Coatings on conventional asphalt can reduce the temperature upto 4°C [48]. Using cool materials to build roads is an effective way of minimizing the effect of urban heat island. Their effectiveness solely depends on surrounding urban area. In our study area, pavements, roads, courtyards and streets will be replaced with the surfaces with progressively higher albedo like New asphalt concrete or reflective concrete [22]. Temperature contours with the existing pavements are shown in Figure 21. Three cases are simulated on 19-Jun-1300 which are given in Table 6 are shown below:

- Reflective Concrete Pavements
- Reflective Building Facades and Walls
- Reflective Coating on both buildings and pavements

Table 8: Using cool pavement materials as a mitigation measure to reduce the average surface temperature

Case	Thermal Diffusivity (mm ² /s)	Albedo	Average Surface Temperature (18 Points)	Difference from Mitigated microclimate
Existing Pavements	1.35	0.32	47.54 °C	0
Reflective Concrete	2	0.5	44.99 °C	2.55
Reflective Building	1.35	0.6	44.54 °C	3
Reflective Coating	1.35	0.6	44.54 °C	3

In the reflective concrete case, all the pavements are replaced with the reflective concrete with absorptivity 0.5 and thermal diffusivity $2 \frac{mm^2}{s}$ and average surface temperature is calculated which is 44.99 °C, this scenario is shown in Figure 22. Next in the reflective building scenario, the albedo of the building walls, facades, roofs and other surfaces are changed to 0.6 with thermal diffusivity by keeping the pavements unchanged. Albedo in the case of reflective coatings is kept 0.6 [49]. In the last two cases, average surface temperature is 44.54 °C which is decreased by 3 °C.

For all the scenarios, the thermal diffusivity and albedo were used to evaluate the roads, façade, roof and walls surface temperatures and comparison was made with the average surface temperature of the 19-Jun-1300.

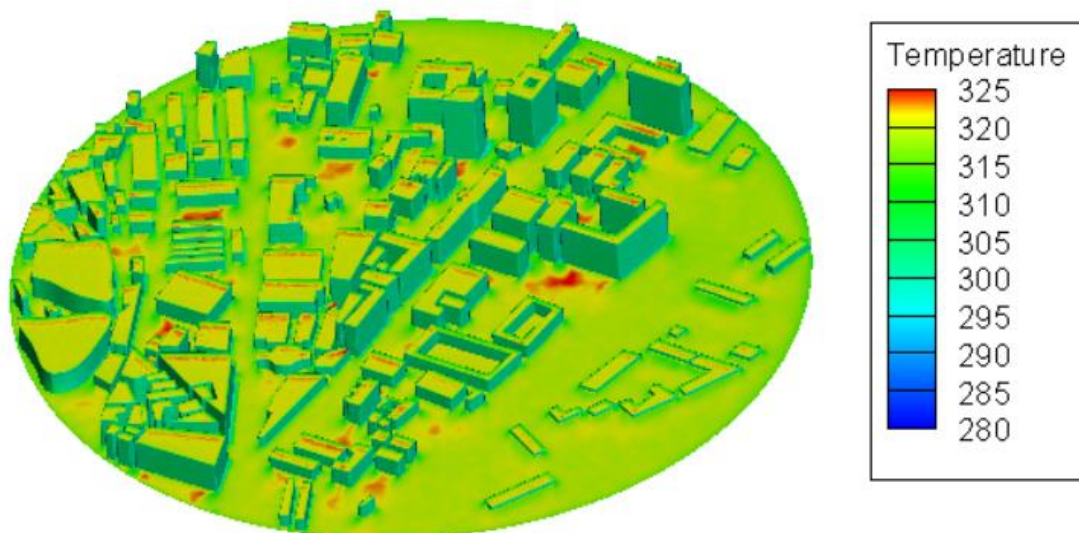


Figure 22:3D View of Temperature Contours of Mitigated Urban Microclimate 19th June 1300

6. Discussion

In this study, in order to conduct the simulation, there were number of processes such as geometrical models and physical processes. Mainly these processes are following:

- Urban 3D model and computational Grid
- Urban Wind Flow through the Study Area
- Solar Radiation Settings in the CFD Software
- Albedo Mitigation Measures at a specific time

6.1 Urban Geometry and Mesh

The Urban Geometry created in this study is based on the satellite imagery and general height data of the buildings available on the web. It was assumed that each floor of the building is nearly 10 ft or 3 meters and height of the building was determined that way as residential buildings in the Karachi are 6 to 8 floors and the commercial buildings are from 6 to 20 Floors with the maximum height building of 102 m. There are elements in the real domain that are not modeled because they do not have major effect on the thermal conditions. Trees, poles, cars and all other obstacles are also neglected and adjusted in the albedo value of the domain. These elements are represented by assigning a solar absorptivity value. All buildings are assumed to have same material and same properties.

Grid generation of this urban domain is explained in detail in the section 3.

6.2 Wind Flow, Solar Radiation and Thermal Model

After the 3D Model is complete, wind velocity settings are selected from the domain and input data. The values for the roughness constants and roughness heights are determined for each boundary. Velocity Profile is kept constant and is expected to develop a profile from the inlet to the circular sub-domain. In this way, wind flow in the urban center is very realistic as possible. Wind Flow of the software was validated using Wind-Tunnel Results.

Thermal conditions for the all building walls are same and also same values are kept for the ground wall conditions. Ground wall is expected to behave as a constant temperature sink with specific thickness. In reality, there are many different regions on the ground with some places with asphalt and some having other material which is ignored to keep the things as simple as

possible. It is assumed that thermal conductivity and specific heat of the surfaces does not change in the simulation or varied with the temperature. Material values are presented in the Table A1. If all the realistic conditions are simulated, it would take a long time for computation and computational cost will be increased. When modeling the solar radiation, the software automatically calculates the sun direction vector from the location and time of the day in a year. The vectors produced are not exact but realistic enough to simulate the region.

In the Section 1, possible reasons for the UHI effect are shown. In this study, few reasons are not modelled which are emissions from industrial source and automobile because it is difficult to model these intricate details. For future studies, it is highly recommended to show all possible causes of the Urban Heat Island Effect in order to improve the accuracy of the simulation. These can be modelled directly or can be added in the computation implicitly by assigning absorptivity values. Modeling of trees and plants are also neglected in this study which contain amount of moisture that can affect the surrounding temperature. It is important in the study areas where this effect is significant, areas near forests or lush green regions.

6.3 Albedo as a Mitigation Measure

In order to reduce the effect of high surface temperature producing thermal discomfort, implementation of reflective pavements, reflective buildings and reflective coatings is suggested which made temperature decreases by 2 to 3 K. For future studies, research must be conducted on the high-albedo and low-cost materials in order to increase pedestrians' comfort.

6.4 Recommendations for further Research

After reviewing the results of the performed simulations and previous literature, following recommendations are made:

- Model the urban environment with more details and fewer buildings
- Keep the upstream and downstream distances high in the simulation
- Compute a transient simulation to gather data more efficiently
- Perform a case with Large Eddy Simulation (LES) rather than realizable k- ϵ model
- Include other sources of UHI in the simulation as well

7. Conclusion

This paper has presented steady CFD simulations considering wind flow and heat transfer including all three modes, investigating the I.I Chundrigar Road region, Karachi. The simulations were performed on ANSYS Fluent using the 3D RANS with k- ϵ turbulence model on a high-resolution grid. For validation of surface temperature, data obtained from satellite products is used. Input conditions were provided by the Meteorological department of Pakistan including wind speed, wind direction, air temperature and solar radiation. Simulations are performed from 18th June until 22nd June 2015. Further, the mitigation of heat stress is performed by changing albedo is simulated. The simulation includes wind flow, solar radiation, average surface temperatures, heat transfer and albedo models. CFD models can provide accurate results if all the guidelines are properly followed. Thus it can be concluded that if higher albedo values of reflective pavements and buildings can reduce the temperature up to 3.0 K

References

- [1] R. WILBY, "A Review of Climate Change Impacts on the Built Environment," *Built Environment*, 2007.
- [2] J. Zuo, S. Pullen, J. Palmer, H. Bennetts, N. Chileshe and T. Ma, "Impacts of heat waves and corresponding measures: a review," *Journal of Cleaner Production*, pp. 1-12, 2015.
- [3] R. P.J., "On the definition of heatwave," *Journal of Applied Meteorology*, pp. 762-775, 2005.
- [4] P. Stott, D. Stone and A. M., "Human contribution to the heat wave of 2003," *Nature*, pp. 610-614, 2004.
- [5] H. L., *Climate of London*, p. 1, 1833.
- [6] A. Synnefa, A. Dandou and M. & M. Tombrou, "On the use of cool materials as a Heat Island Mitigation Strategy," *American Meteorological Society*, pp. 2846-2856, 2008.
- [7] M. Nuruzzaman, "Urban Heat Island: Causes, Effects and Mitigation Measures - A Review," *International Journal of Environmental Monitoring and Analysis*, pp. 67-73, 2015.
- [8] T. Oke, "City Size and the Urban Heat Island," *Atmospheric Environment*, pp. 769-779, 1973.
- [9] A. Rosheida and H. Bryan, "Optimizing the effect of vegetation for pedestrian thermal comfort and urban heat island mitigation in a hot arid environment," in *Fourth National Conference of IBPSA-USA*, New York, 2010.
- [10] T. Oke, "The Energetic Basis of the Urban Heat Island," *Quarterly Journal of the Royal Meteorological Society*, pp. 1-24, 1982.
- [11] Q. u. Z. Chaudhry, "Climate Change Profile of Pakistan," Asian Development Bank, 2017.
- [12] M. Zahid and G. Rasul, "Rise in Summer Heat Index over Pakistan," *Pakistan Journal of Meteorology*, p. 6(12), 2010.
- [13] S. Saijd, B. Hussain, M. A. Khan, A. Raza, B. Zaman and I. Ahmed, "On rising temperature trends of Karachi in Pakistan," *Climatic Change*, pp. 539-547, 2009.
- [14] D. Q. u. Z. Chaudhry, D. G. Rasul, A. Kamal, M. A. Mangrio and S. Mahmood, "Technical Report on Karachi Heat Wave June 2015," Ministry of Climate Change, Karachi, 2015.
- [15] E. Tribune, "Improvement of II Chundrigar Road to start soon," 4 August 2019. [Online]. Available: <https://www.tribune.com.pk/2027661/1-improvement-ii-chundrigar-road-start-soon/>. [Accessed 1 May 2020].
- [16] J. Franke, A. Hellsten, H. Schlunzen and B. Carissimo, Best Practice Guideline for the CFD Simulation of flows in the Urban Environment, Hamburg, Germany: University of Hamburg, 2007.

- [17] B. Blocken, "Computational Fluid Dynamics for Urban Physics: Importance, scales, possibilities, limitations and ten tips and tricks towards accurate and reliable simulations," *Building and Environment*, pp. 1-27, 2015.
- [18] Y. Toparlar, B. Blocken, B. Maiheu and G. v. Heijst, "A review on the CFD analysis of urban microclimate," *Renewable and Sustainable Energy Reviews*, 2017.
- [19] H. Mittal, A. Sharma and A. Gairola, "A review on the study of urban wind at the pedestrian level around buildings," *Journal of Building Energy*, 2018.
- [20] W. Janssen, B. Blocken and T. v. Hooff, "Use of CFD simulations to improve the pedestrian wind comfort around a high rise building in a complex urban area," in *13th Conference of International building performance Simulation Association*, Chambéry, France, 2013.
- [21] Y. Toparlar, B. Blocken, P. Vos, G. v. Heijst, W. Janssen and T. v. Hooff, CFD Simulation and validation of urban microclimate: A case study for Bergpolder Zuid, Rotterdam, Eindhoven: Building and Environment, 2014.
- [22] S. Sen, J. Roesler, B. Ruddell and A. Middel, "Cool Pavement Strategies for Urban Heat Island Mitigation in Suburban Phoenix, Arizona," *Sustainability*, 2019.
- [23] L. S. Rose and R. Levinson, "Analysis of the effect of vegetation on albedo in residential areas: case studies in suburban sacramento and Los Angeles, CA," *GIScience & Remote Sensing*, pp. 64-77, 2013.
- [24] M. Santamouris, N. Gaitani, A. Spanou, M. Saliari, K. Giannopoulo and K. Vasilakopoulo, "Using Cool Paving Materials to improve microclimate of Urban Areas - Design realization and results of the flisvos project," *Building and Environment*, pp. 128-136, 2012.
- [25] S. Firdaus Fatima and C. H. Nasarullah, "Steady-state CFD modelling and experimental analysis of the local microclimate in Dubai (UAE)," *Sustainable Buildings*, 2017.
- [26] K. Setia, N. Hamza, M. Mohammed, S. Dudek and T. Townshend, "CFD Modeling as a tool for assessing outdoor thermal comfort conditions in urban settings in hot aird climate," *Journal of Information Techonology construction*, pp. 19,248, 2014.
- [27] S. Liu, W. Pan, H. Zhang, X. Cheng, Z. Long and Q. Chen, "CFD Simulations of wind Distribution in an urban community with a full-scale geometrical model," *Building and Environment*, pp. 11-23, 2017.
- [28] O. SATIR, "Defining the Plantation Role to mitigate the Urban Heat Island Effects on Global Warming using Thermal Satellite Sensor," in *International Conference on Advanced Technology & Sciences (ICAT'16)*, Konya, 2016.
- [29] R. Ramponi, B. Blocken, L. B. d. Co and W. Janssen, "CFD Simulation of outdoor ventilation of generic urban configurations with different urban densities and equal and unequal street widths," *Building and Environment*, 2015.
- [30] A. d. L. Vollaro, G. d. Simone, R. Romagnoli, A. Vallati and S. Botillo, "Numerical Study of Urban Canyon Microclimate related to geometrical parameters," *Sustainability*, pp. 7894-7905, 2014.

- [31] S. Bottilo, A. D. L. Vollaro, G. Galli and A. Vallati, "Fluid Dynamic and Heat Transfer in an urban canyon," *Solar Energy*, pp. 1-10, 2014.
- [32] S. M. Salim, R. Buccolieri, A. Chan and S. D. Sabatino, "Numerical Simulation of atmospheric pollutant dispersion in an urban street canyon: Comparison between RANS and LES".
- [33] ANSYS, ANSYS Fluent Theory Guide, Canonsburg: ANSYS, Inc, 2013.
- [34] A. Jakeman and J. N. R.A. Letcher, "Ten iterative steps in development and evaluation of environmental models," *Environmental Modelling & Software*, pp. 602-614, 2006.
- [35] J. FRANKE, A. HELLSTEN, H. SCHLUZEN and B. CARISSIMO, "The Best Practise Guideline for the CFD Simulation of flows in the urban environment : an outcome of COST 732," in *Chapel Hill*, North Carolina, 2010.
- [36] Y. Tominaga, A. Mochida, R. Yoshie, H. Kataoka, T. Nozu, M. Yoshikawa and T. Shirasawa, "AJI Guidelines for Practical Applications of CFD to pedestrian Wind Environment around buildings," *Journal of Wind Engineering and Industrial Aerodynamics*, pp. 1749-1761, 2008.
- [37] W. B.G., "A Wind Tunnel Study of Wind Velocities in passage between and through buildings," in *Proceedings of the 4th International Conference on Wind Effects on Buildings*, Heathrow, 1975.
- [38] J. Allegrini, V. Dorer and J. Carmeliet, "Buoyant Flows in Street Canyons: Validation of CFD simulations with wind tunnel measurements," pp. 63-74, 2014.
- [39] F. BAETKE, H. WERNER and WENGLER, "Numerical Simulation of Turbulent Flow over surface mounted obstacles with sharp edges and corners," *Journal of Wind Engineering and Industrial Aerodynamics*, pp. 129-147, 1990.
- [40] "PointWise," Pointwise, Inc., [Online]. Available: <https://www.pointwise.com>. [Accessed 16th January 2020].
- [41] Ramponi and Blocken, "CFD Simulation of cross-ventilation for a generic isolated building; impact of computational parameters," *Building and Environment*, pp. 34-48, 2012.
- [42] J. Wieringa, "Updating the Davenport Roughness Classification," *Journal of Wind Engineering and Industrial Aerodynamics*, pp. 357-368, 1992.
- [43] P. S. REITER, "Validation Process for CFD Simulations of Wind Around Buildings," in *European Built Environment CAE Conference*, Belgium, 2008.
- [44] NASA, "MODIS," 18 June 2015. [Online]. Available: <https://modis.gsfc.nasa.gov/data/dataproduct/mod11.php>. [Accessed 18 Dec 2019].
- [45] V. F. Vazquez, F. Teran, J. Luong and S. E. Paje, "Functional Performance of Stone Mastic Asphalt Pavements in Spain : Acoustic Assessment," *Coatings*, 2019.
- [46] S. ONDER and A. AKAY, "The Roles of Plants on Mitigating the Urban Heat Islands' Negative Effects," *International Journal of Agriculture and Economic Development*, pp. 18-32, 2014.
- [47] G. L. Feyisa, K. Dons and H. Meilby, "Efficiency of parks in mitigating urban heat island effect: An example from Addis Ababa," *Building and Environment*, pp. 87-95, 2014.

- [48] N. A. A. Guntor, M. F. M. Din, M. Ponraj and K. Iwao, "Thermal Performance of Developed Coating Material as Cool Pavement Material for Tropical Regions," *Journal of Materials in Civil Engineering*, 2014.
- [49] H. Li, A. Saboori and X. Cao, "Information Synthesis and Preliminary Case Study for life cycle of reflective coatings for cool pavements," *International Journal of Transportation Science and Technology*, pp. 38-46, 2016.
- [50] TecPlot, TecPlot User Manual, Bellevue, 2016.
- [51] A. d. L. Vollaro, G. Galli and A. Vallati, "CFD analysis of Convective Heat Transfer Coefficient on External Surfaces of buildings," *Sustainability*, pp. 9088-9099, 2015.

Appendix

Table A1: Material Specifications of the Computational Domain in SI Units

Material	Density	Specific Heat	Thermal Conductivity	Absorptivity	Emissivity
Earth	1150	650	1.5	0.68	0.9
Brick	1400	900	1.7	0.5	0.88

Table A2: Raw Surface Temperature Data from CFD Results of 15 Points of 13 cases of Study Area

18th-0900	18th-1400	18th-1600	19th-1000	19th-1300	19th-1600	19th-1800	20th-0900	20th-1600	21st-0900	21st-1500	22nd-0700	22nd-1300
310.25	317.88	309.26	308.87	320.84	309.41	297.91	312.45	299.4	308.06	312.91	295.01	315.26
310.37	317.48	306.42	312.87	321.67	309.72	294.91	313.45	305.6	308.15	315.52	295.94	314.01
310.84	317.25	318	312.69	321.35	310.1	294.22	313.42	306.72	307.95	316.43	295.922	311.27
309.13	317.85	305.58	313.99	320.99	310.4	294.06	312.46	308.46	307.05	314.37	295.91	311.42
309.63	313.06	314.77	314.17	320.43	310.19	294.03	312.71	306.4	308.08	314.67	295.08	310.86
309.53	312.54	315.83	314.24	320.46	310.56	295.21	312.79	300.32	308.91	315.23	295.96	318.48
309.28	317.67	314.62	314.2	320.01	310.33	294.9	312.68	299.85	308.95	314.67	295.05	318.52
308.92	317.1	314.37	313.72	319.78	310.577	294.66	312.66	309.73	308.93	315.07	295.81	306.72
309.44	317.8	315.03	312.76	320.43	310.88	294.24	313.01	309.91	309.91	315.22	295.83	312.82
308.88	318.37	314.54	312.42	320.78	311.01	294.95	312.11	307.61	307.99	315.52	295.99	315.29
310	316.95	314.77	313.32	321.12	310.69	294.88	312.55	309.56	307.94	314.81	296.01	309.82
310.97	316.93	314.64	312.01	320.06	311.65	295.01	312.44	307.24	308.81	314.8	295.43	319.87
311.15	317.35	314.67	314.84	320.07	311.79	295	312.23	307.81	309.01	315.01	295.01	318.63
311.56	317.12	313.69	308.81	319.59	311.88	295.22	312.91	309.24	308.33	315.33	295.11	318.01
309.996	316.810	313.299	312.779	320.541	310.656	294.942	312.705	306.275	308.4336	314.96857	295.57586	314.35571

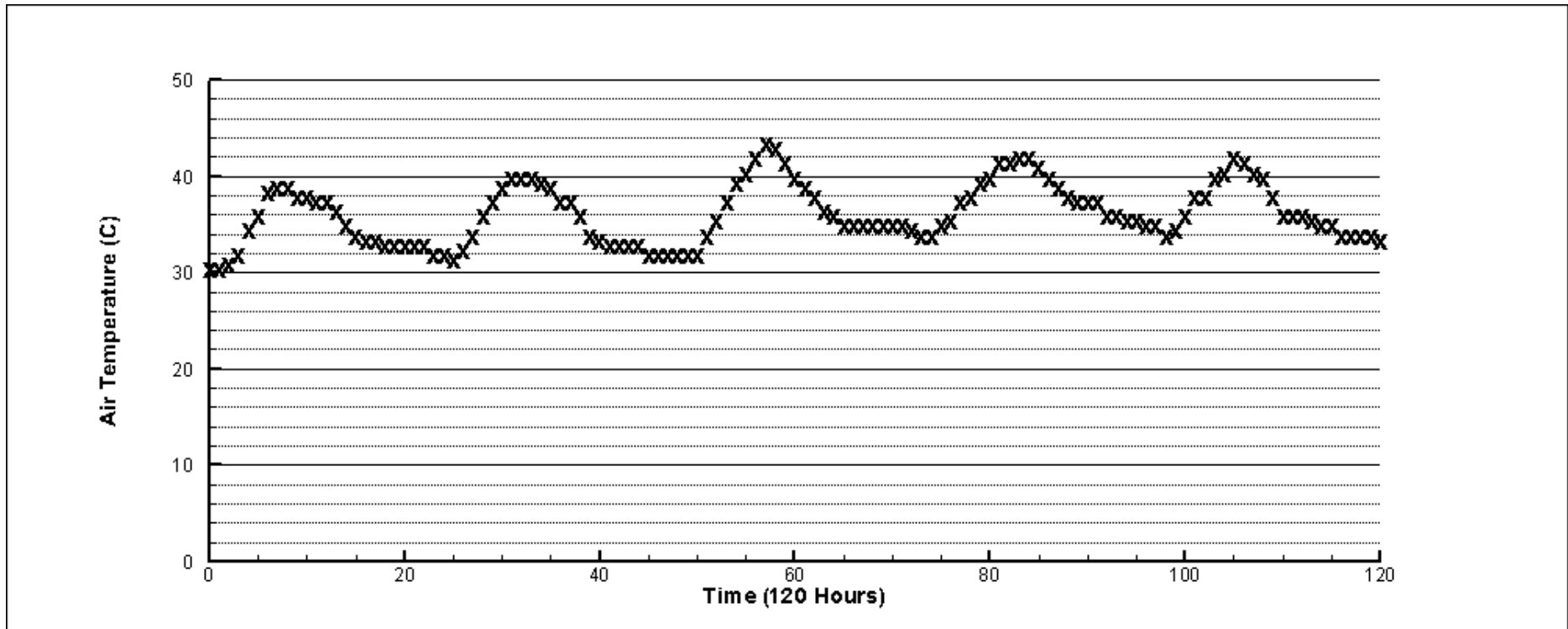


Figure 23: Air Temperature vs Time from 18th June to 22nd June 2015

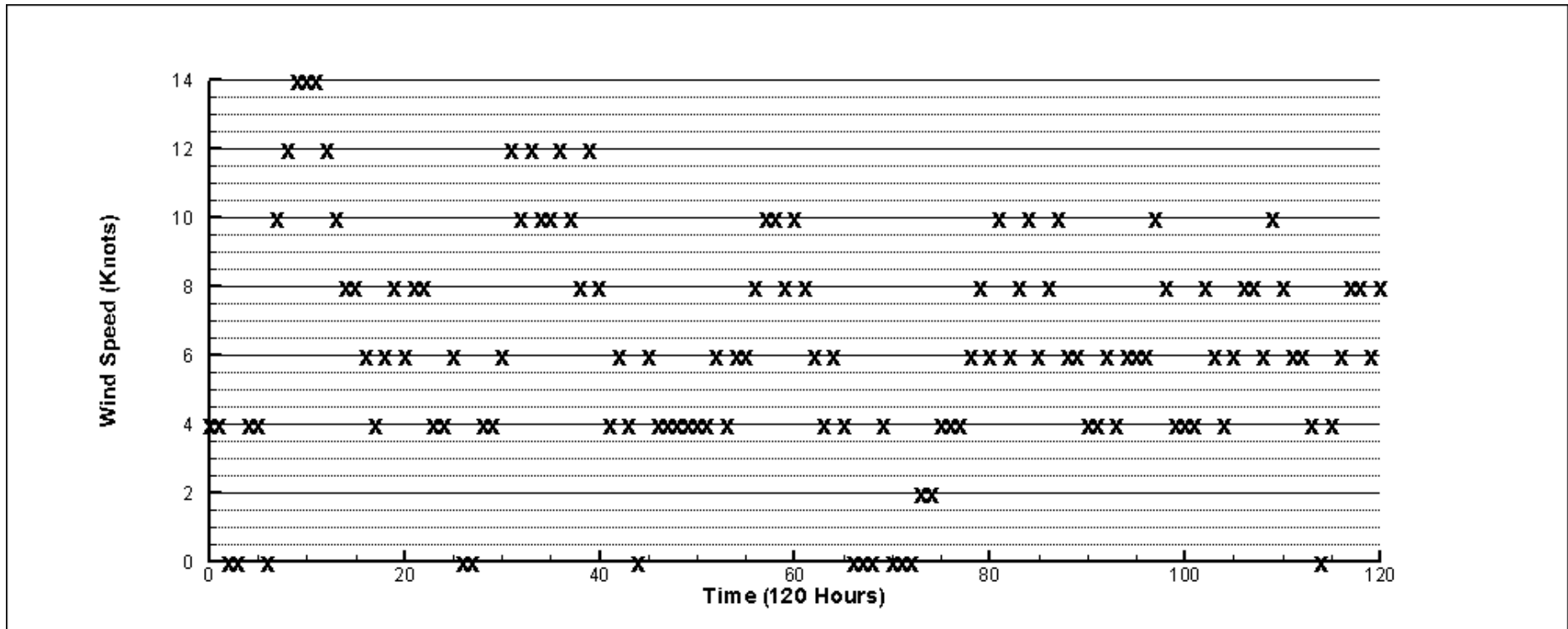
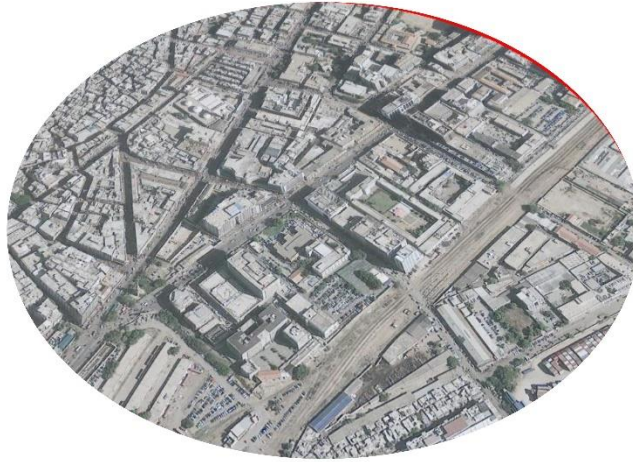
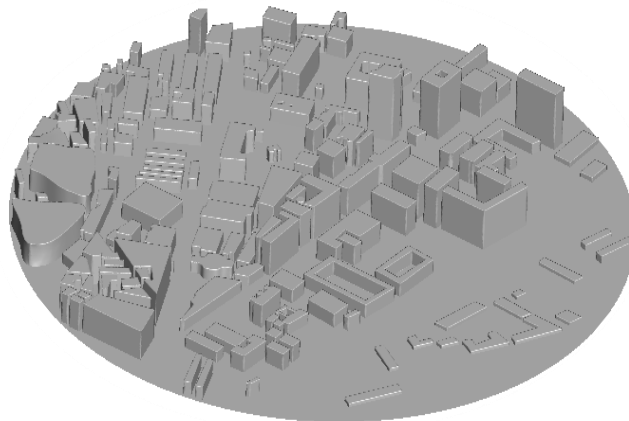


Figure 24: Wind Speed vs Time from 18th June to 22nd June 2015

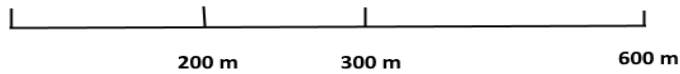
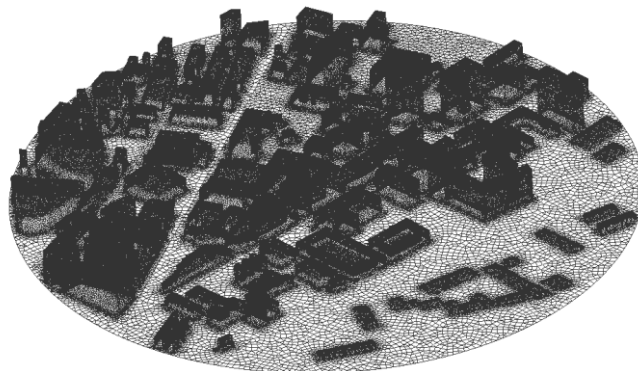
a)

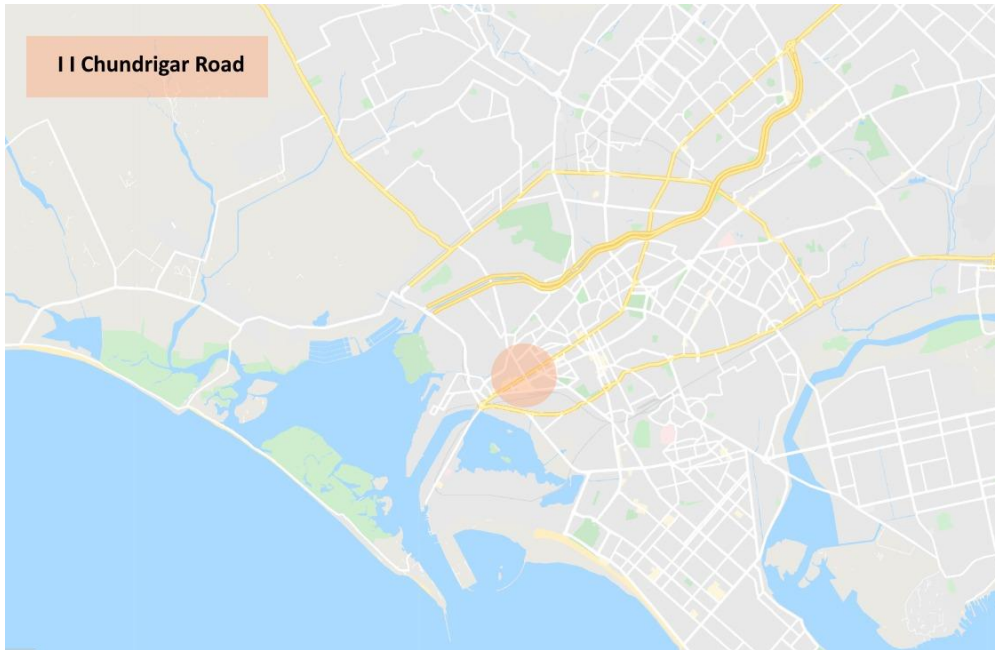


b)



c)





b)

